

NOTE: Revised Post-WPTT14 meeting

A hierarchical Bayesian integrated model incorporated direct ageing, mark-recapture and length-frequency data for yellowfin (*Thunnus albacares*) and bigeye (*Thunnus obesus*) of the Indian Ocean

Dortel E.¹, Sardenne F.², Le Croizier G.², Million J.³, Hallier J.P.¹, Morize E.²
Munaron J.M.², Bousquet N.⁴, Chassot E.¹

¹ *Institut de Recherche pour le Développement, UMR 212 EME, Avenue Jean Monnet, BP 171, 34 203 Sète cedex, FRANCE*

² *Institut de Recherche pour le Développement, UMR 6539 LEMAR, BP70, 29 280 Plouzané, FRANCE*

³ *Indian Ocean Tuna Commission, PO Box 1011, Victoria, SEYCHELLES*

⁴ *EDF Research and Development, Department of Industrial Risk Management, 6 quai Watier, 78 401 Chatou, FRANCE*

Abstract. Despite several studies conducted in the 3 oceans, the shape and parameterization of yellowfin and bigeye growth curves are still open to debate. In this study, we present an integrated growth model that combines mark-recapture and direct ageing data from saggital otoliths collected through the Indian Ocean Tuna Tagging Program (RTTP-IO) and the West Sumatra Tuna Tagging Project (WSTTP) as well as length-frequency data sampled from the European purse seine fishery over the last decade. Developed in a Bayesian framework, the model accounts for uncertainty in age estimates and includes ancillary information derived from expert judgment on otolith reading as well as from data on sex and observed maximum size of fish individuals. Our results confirm the existence of 2 stanzas for the growth of yellowfin and bigeye during exploitation phase.

Key words: Yellowfin; Bigeye; integrated growth model; Bayesian framework

1 Introduction

Fish growth is a key biological parameter in fisheries research. Determining mean population growth as well as variability among individuals are essential to understand the productivity of fish populations and their ability to resistance to environmental change and fishing pressure. Growth curves are used as input, directly or indirectly, into the stock assessment models to estimate the age composition of the commercial catches and supply the scientific advice on stock status.

Different sources of information for studying fish growth are available, (i) direct ageing of a fish of known size from periodic deposits in calcified and skeletal tissues, such as scales, vertebrae, otoliths, and spines, (ii) increase in fish length over the time-at-liberty from mark-recapture experiments, (iii) modal progressions in length-frequency distributions from commercial catches or scientific monitoring. These different data sources provide additional informations on different life cycle stages and therefore on growth phases and it may be difficult to obtain an overall growth pattern from a single data source. However, although many studies have been conducted on fish growth, only few studies have attempted to combine the different information sources in an integrated growth model (Eveson et al., 2004; Restrepo et al., 2010).

Yellowfin tuna (*Thunnus albacares*, Bonnaterre 1788) and bigeye tuna (*Thunnus obesus*, Lowe 1839) are epipelagic species widely distributed in the tropical and subtropical waters of the major oceans. In the Indian Ocean (IO), these tuna stocks are exploited by a large diversity of fishing fleets from industrial fleets dominated by longline and purse seine to artisanal fleets (Herrera and Pierre, 2010) and the induced effects are very important for the economic development of Indian coastal States. Therefore, it is necessary to conciliate a sustainable management of the stock with the economic constraints encountered by these countries.

The management of Indian Ocean tunas stocks are under the jurisdiction of the Indian Ocean Tuna Commission (IOTC) and relies on the assessment of the stock status through age-structured population dynamics models (Langley et al., 2010). The age-structure in commercial fisheries catches is assessed from the length-structure using an age-length key derived from growth parameters. Nevertheless, much uncertainty currently remains on the growth to be considered in yellowfin and bigeye stock assessments. Growth of the Indian Ocean yellowfin has been the focus of several studies based on modal progression analysis (Marsac and Lablache, 1985; Marsac, 1991; Lumineau, 2002; Viera, 2005) and direct ageing (Le Guen and Sakagawa, 1973; Romanov and Korotkova, 1988; Stéquent, 1995) leading to conflicting results due to differences in sampling, gear selectivity, and estimation methods historically raised issues about the shape of the growth curve and its parameterization. Historical studies on yellowfin growth relied on the classical Von Bertalanffy model (1938), assuming a constant growth rate over the full lifespan of the fish, while most recent studies support a two-stanza growth curve characterized by a significant change in growth rate between juveniles and adults (Gascuel et al., 1992; Lehodey and Leroy, 1999; Lumineau, 2002). In addition, modal progression and direct ageing data have specific features and biases, which makes difficult the comparison of growth curves obtained from a single data source. Growth bigeye has been little study

(Chantawong et al., 1999; Stéguert and Conand, 2004) and remain poorly known. Preliminary studies of data collected throughout the RTTP-IO, including otolith and tag-recapture, supported a two-stanza growth pattern both for yellowfin and for bigeye characterized by a slowdown during their juvenile phase (Fonteneau and Gascuel, 2008; Eveson and Million, 2008; Morize et al., 2008). Most stock assessments consider a mean growth pattern and static parameter estimates. The range of uncertainty as well as individual variability are ignored which result in substantial biases in estimates of stock productivity or its resilience to fishing (Punt and Hilborn, 1997) and eventually modifies the perception of stock status and associated management advice. The first source of variability in growth might arise from a sexual dimorphism. For Indian Ocean yellowfin, several authors showed that males become largely dominant above 145 cm F_L (Nootmorn et al., 2005; Zhu et al., 2008; Zudaire et al., 2010). According to Wild (1986), in the eastern Pacific, the yellowfin females faster growth than the male until 94.9 cm F_L (at about 2 years) then the trend reverses. For Pacific Ocean bigeye, the ratio of males increases from 120 cm F_L and reached 75% over 170 cm (Kume and Joseph, 1966).

Since the 1990s, Bayesian modelling approaches have gained growing interest in applied ecology and environmental sciences (Clark, 2005). The Bayesian framework offers the advantage of incorporating into the statistical data analysis some expert judgment and ancillary information in a rigorous and consistent manner (Gelman et al., 2004; Cressie et al., 2009). This is particularly suitable in fisheries science where data are almost always partially observed with measurement errors or uncertainties. Bayesian models have been used to make inferences about fish growth (Helser and Lai, 2004) so as to provide scientific advice for fisheries management (Punt and Hilborn, 1997; McAllister et al., 2001; Chen et al., 2003).

In this study, we present an integrated growth model that combine mark-recapture and otolith readings collected through the Indian Ocean Tuna Tagging Program (RTTP-IO), as well as otoliths collected during the West Sumatra Tuna Tagging Project (WSTTP), and length-frequency data sampled from the European purse seine fishery over the last decade. Developed in a hierarchical Bayesian framework, a flexible approach to exploit diverse sources of information that complement each, the model accounts for uncertainty in age estimates and length measurements and includes ancillary information derived from expert judgment on otolith reading. In a first part, the integrated model is used to provide robust estimates of growth of Indian Ocean yellowfin and bigeye tunas. Then, the model results are used to highlight a sexual dimorphism of growth from a sub-sample of data.

2 Materials and Methods

2.1 Data collection

2.1.1 Mark-recapture data

Mark-recapture data were collected throughout the Regional Tuna Tagging Project (RTTP-IO). This tagging were carried out by IOTC during 2005-2007 on 3 pole-and-line vessels chartered to operate in the Western Indian Ocean and off western Indonesia. In addition, from 2002 to 2009, the IOTC released 31,455 tunas during one-shot operations (Maldives, Laccadive, Andaman, Indonesia, Mayotte, Eastern Indian Ocean). Field operations consisted in catching tunas, tagging them on a vinyl-covered cradle, measuring their fork length (fish length from the front to the fork in the center of the tail; F_L) through graduations directly printed on the cradle and releasing them at sea (Hallier, 2008). Date and geographic location were recorded for each tag event. A total of 64,323 yellowfin and 34,960 bigeye were tagged with HallprintTM dart tags inserted into the musculature, below the second dorsal fin. In addition, 2,741 yellowfin and 2,443 bigeye were also chemically tagged with oxytetracycline (OTC), an antibiotic that is rapidly incorporated into calcified parts such as bones, scales, and otoliths and leaves a permanent fluorescent mark in the growth increment being formed at the time of tagging. According to fish size, 1.5-3 mL of OTC were injected with a syringe in the intramuscular part of their back (Hallier, 2008).

Recovery operations took place in the whole basin of the Indian Ocean during 2005-2012. Most of the reported recoveries came from fish caught by the European purse-seine (IOTC 2011). In September 2012, 10,395 yellowfin and 5,639 bigeye had been recovered. F_L of recovered fish was measured with caliper or tape measure to the nearest 0.5 cm. The accuracy in date and location of recaptures is dependent on place and process in which the tag is recovered. About 20% of the recoveries were made during purse seine fishing operations which resulted in the recovered fish to be associated with one position and date. By contrast, tunas recovered during purse seine unloading could be associated with several dates and locations of catch due to the process of storing tunas in refrigerated wells which contain about 5 sets over a fishing trip. The recovery can also occur downstream of the unloading process or in the canneries. The range of dates associated with each recapture was derived from logbook data and well maps through close collaboration between the IOTC and the purse seine fishing industry.

Some selection criteria have been applied to this mark-recapture data leading to a reliable dataset:

- Fish for which the species recorded at tagging differs from the species at recovery were excluded.
- At tagging, all fish are measured in fork length whereas at recovery the length measurement may correspond to fork length, first dorsal length or curve length, the two latter being converted in fork length. This conversion is considered imprecise so these data were excluded.

- Fish for which length measurement at tagging or at recovery was reported as unreliable by the RTTP-IO team were excluded.
- Fish with a negative growth rate between tagging and recapture were excluded.
- Fish whose date of recovery was unknown or known with low accuracy, i.e. $> 5\%$, were excluded.
- The dart-tagged fish that spent less than 90 days at sea and the OTC-tagged fish that spent less than 30 days at sea were excluded.
- The tag recovery system has evolved over the RTTP-IO program. Dates, positions and size measurements of recovery prior to 2007 being considered as low reliable, these observations have not been preserved.

In addition to these criteria, only yellowfin for which the exact recapture date was known and bigeye for which the recapture date was known with an uncertainty of 7 days were used for modeling growth. Finally we obtained a dataset composed of 2,068 yellowfin (Appendix C., Fig. C.1) and 2,655 bigeye (Fig. C.2).

On the other hand, sex was identified for some fish of RTTP-IO program. These fish constituted an independent mark-recapture dataset comprising 34 females of 47 to 71 cm F_L at tagging and 106 to 147.1 cm F_L at recapture and 54 males of 42 to 100 cm F_L at tagging and 116 to 161 cm F_L .

Table 1: Summarize of RTTP-IO data selections

* Correspond to chemically tagged fish with oxytetracycline (OTC)

| | | Yellowfin | | Bigeye | |
|---------------------------|------------------------|-----------|--------|--------|--------|
| Number of tagged fish | All data | 66,534 | 2,756* | 35,995 | 2,443* |
| | Selected tagging data | 64,323 | 2,741* | 34,960 | 2,425* |
| Number of recaptured fish | All data | 10,505 | 257* | 5,639 | 196* |
| | Selected tagging data | 10,395 | 256* | 5,583 | 192* |
| | Selected recovery data | 4,464 | 174* | 2,940 | 145* |
| | Data used | 2,068 | 128* | 2,655 | 85* |

2.1.2 Direct ageing data

Currently, 256 yellowfin and 192 bigeye tagged with OTC have been recaptured. Sagittal otoliths were collected for ageing from 128 yellowfin, of 43 to 72 cm F_L at tagging and 47.9 to 135.4 cm F_L at recapture and from 85 bigeye of 44 to 71.5 cm F_L at tagging and 46 to 141.6 cm F_L at recapture. Otoliths were extracted, rinsed in water to remove tissue, and stored dry.

For the yellowfin, additional information to the RTTP-IO data were included: (i) 18 fish of 19 to 29 cm F_L captured during the tagging operations of the West Sumatra Tuna Tagging Project (WSTTP) carried out by the IOTC August 2007 and (ii) 42 fish captured in 2008 and 2009 by the

Indian Ocean Tuna Ltd (IOT) including 7 males of 123.1 to 145 cm F_L , 7 females of 94.1 to 147.5 cm F_L and 28 indeterminate fish of 31 to 128.7 cm F_L .

Yellowfin have fragile, thin, and elliptic otoliths that require particular care during preparation and interpretation of microstructural features (Wild and Foreman, 1980). All otoliths collected were analysed at the "Laboratoire de Sclérochronologie des Animaux Aquatiques" (LASAA) in Brest, France. Otoliths were prepared for age analysis following methods described elsewhere (Secor et al., 1991; Stéquent, 1995; Panfili et al., 2002). They were cleaned in sodium hypochlorite and rinsed with distilled water before being embedded in resin block and transversally cut on both sides of the nucleus. The section containing the nucleus was then fixed to a glass slide using thermoplastic glue and sanded to the level of the nucleus using different alumina grains (0.3 to 3 μm). The operation was performed on each side of the section until a slice of about 100 μm thickness was decalcified with EDTA (tri-sodium-ethylene-diaminetetraacetic acid) to increase contrast between increments. The thin slides were examined under a microscope (1000x magnification) for counting increments throughout the counting path on the sagitta, i.e. from the primordium, or point of original growth, to the last increment deposited on a maximal growth axis.

Otoliths collected from fishes not chemically tagged were read in full, i.e. between the nucleus and edge (Ir). For the OTC-tagged yellowfin, the number of increments was counted for different otolith sections: (i) between nucleus and OTC mark (It), (ii) between the OTC mark and edge (Im) and (iii) between the nucleus and edge (Ir) (Fig. 1). For the OTC-tagged bigeye, the number of increments was counted for the sections Im and It . Each otolith was read 2-5 times without prior knowledge on size or time-at-liberty of the individuals sampled so as to maintain certain independence between the multiple readings. Otolith readings were performed by two reader teams.

2.1.3 Modal progression from length-frequency data

Length-frequency data come from the "Balbaya" database managed by the "Institut de Recherche pour le Développement" (IRD, Sète) and correspond to commercial catches of European, Seychelles, Iranian and Mayotte purse-seine vessels. These catches were conducted under FAD-associated school and free school between December 2000 and March 2010 in three fishing areas, i.e. Southeast and Northwest Seychelles and Sud Somali (Fig. 2).

These length-frequency distributions exhibit various modes corresponding to different cohorts whose the progression in length was tracked monthly. An analytical method of modes separation was used. This latter describes the length distributions of the various cohorts, in a given month, as a mixture of normal distributions (Hasselblad, 1966; Schnute and Fournier, 1980). The modal determination was performed with the mix function, mixdist package of R statistical software version 2.12.2, that fits a set of overlapping component distributions to monthly length-frequency histograms using an Expectation-Maximization algorithm (Macdonald and Green, 1988). This function requires starting values for means and standard deviations. To optimize their choice, the normalmixEM function of

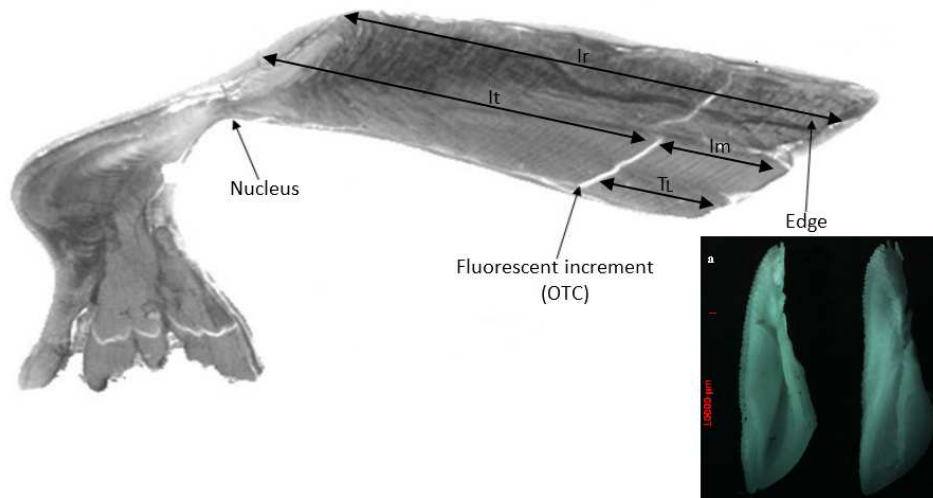


Figure 1: Otoliths of yellowfin tuna (external right and internal left) and the different sections used for reading the number of increments; OTC: Oxytetracycline; *It*: section from the nucleus to the OTC mark; *Im*: section from the OTC mark to the edge; *Ir*: section from the nucleus to the edge; *T_L*: Time-at-Liberty

mixtools package was used. Owing to a slower growth for larger fish and an increase of individual variability in size-age relationship with increasing age, especially after the sexual maturity, overlaps between successive length-at-age distributions increases and makes the visually identification of modes increasingly difficult. So, the standard deviation was constrained to increase with the mean value.

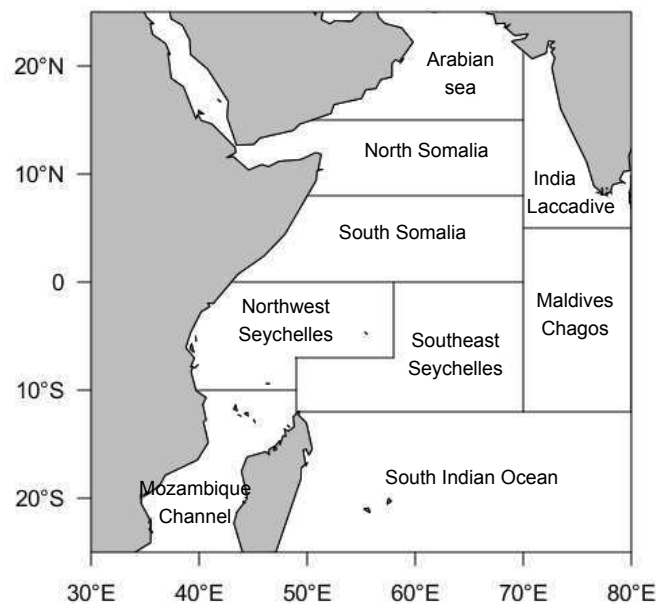


Figure 2: Fishning areas of Indian Ocean

Yellowfin and bigeye have a seasonal sexual activity and thus display conspicuous recruitment peaks. The Indian Ocean yellowfin has two spawning season, the main from November to March with a peak in January and a minor period, involving a smaller number of spawning females, from June to August with a peak in June-July (Stéquent et al., 2001; Zhu et al., 2008). The juveniles are mainly recruited during August to October and February to March. The reproduction of bigeye occurs in December to January and around June (Nootmorn, 2004) and the juveniles are mainly recruited during August to September and January to March. Therefore, an average age with an uncertainty of 3-4 months can be attributed to length modes. 23 cohorts and 16 cohorts were identified for yellowfin and bigeye respectively. But, due to lack of fish in intermediate sizes, it was impossible to follow the cohorts over 73 cm F_L for yellowfin and 115 cm F_L for bigeye (Fig. 3).

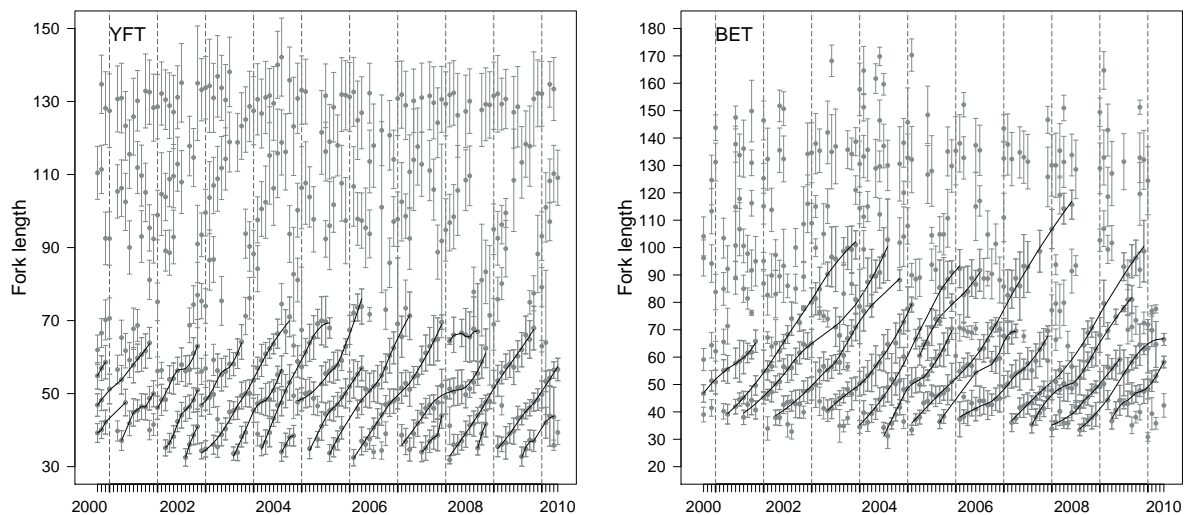


Figure 3: Monthly modal position in length-frequencies from purse seiners catches for yellowfin (YFT) and bigeye (BET). The circles represent the mode position and the vertical line the standard deviation; the solid curves correspond to the progression of identified cohorts

2.2 Modelling growth

2.2.1 Choice of growth model

A hierarchical Bayesian model in which growth varies according to an individual-specific stochastic process was implemented. Preliminary analysis of the RTTP-IO data (Eveson and Million, 2008; Fonteneau and Gascuel, 2008) indicated a succession of phases of growth deceleration and acceleration in the growths of yellowfin and bigeye tunas. So, we considered the VB logK model, a two-stanza growth model developed by Laslett et al. (2002) for the growth of southern bluefin tuna. This model allows a smooth transition between two different growth rate coefficients (k_1 and k_2)

through modeling changes in growth by a logistic function (Laslett et al., 2002; Eveson et al., 2004). The expected fork length at age A is expressed as:

$$f(A - t_0, \theta_g) = L_\infty(1 - \exp(-k_2(A - t_0))) \times \left(\frac{1 + \exp(-\beta(A - t_0 - \alpha))}{1 + \exp(\beta\alpha)} \right)^{\frac{(k_1 - k_2)}{\beta}} \quad (1)$$

All parameters used in this relation are defined in Table A.1.

Table 2: Parameters and variables used in the somatic growth models

| Variable | Definition |
|-------------------------|--|
| $L_{i,j}$ | Fork length, i.e. length from the front to the fork in the center of the tail, for fish i at opportunity of capture j (cm) |
| $A_{i,j}$ | Age of fish i at opportunity of capture j (year) |
| $\mu_{c,k}$ | Fork length mode for cohorte c at month k (cm) |
| $a_{c,1}$ | Initial age for the cohorte c (year) |
| L_∞ | Asymptotic fork length (cm) |
| k_1 | Juvenile growth rate coefficient (year ⁻¹) |
| k_2 | Adult growth rate coefficient (year ⁻¹) |
| α | Inflection point between the 2 stanzas (year) |
| β | Transition rate between k_1 and k_2 |
| t_0 | Theoretical age at fork length 0 (year) |
| $\varepsilon_{i,j}$ | Length measurement error for fish i at opportunity of capture j (cm) |
| $\varepsilon_{\mu c,k}$ | Modal length uncertainty for the cohort c at month k (cm) |
| λ_i | Adjustement parameter for mark-recapture data (year); for fish i , $\lambda_i = t_0 + \alpha - A_{i,1}$ |

2.2.2 Fitting to direct ageing data

The tunas otoliths are particular difficult to read and the age estimation involves subjective interpretations of reader and comprises some uncertainties which can result in bias in growth estimate. Errors in interpreting and counting daily increments can first be related to otolith preparation for reading. In particular, some increments may be “lost“ at the otolith nucleus (i.e. core) and edge. Otoliths can also exhibit discontinuities and zones of overlap that result in some increments being omitted or counted more than once. Reading errors generally increase for older fish because the number of increments to count increases and because increments tend to get narrower with the distance from the nucleus when the fish is approaching its asymptotic length (Uchiyama and Struhsaker, 1981; Stéquent, 1995). In addition, growth increments might not always be consistently deposited daily, i.e. sub-daily increments and discontinuities in accretion rate may occur due to stress, reproduction, and environmental conditions, which may result in biased age estimates (Radtke and Fey, 1996; Panfili et al., 2009).

Therefore, a ageing error was used to estimate the individual ages of fish (Dortel et al., prep).

Developed in a Bayesian framework, it explicitly considered the sources of uncertainty associated with otolith reading. In a first model step, the hypothesis of daily increment deposition (Wild and Foreman, 1980; Wild et al., 1995) was tested based on a subset of data of OTC-tagged otoliths. The information on the process of increment deposition was subsequently used in a second step for estimating the age of each fish based on counts of otolith increments. Expert judgment was included in the ageing error model through the choice of stochastic error structure and elicitation of informative prior density functions (Appendix A).

The somatic VB log K growth model (Eq.11) was coupled to the ageing error model so as to propagate age uncertainty into growth parameter estimates and fitted to the data using Bayesian inference. The observed fork length of fish i at the opportunity of capture j , i.e; $j = 1$ at tagging and $j = 2$ at recapture, was then modeled as:

$$L_{i,j}^* = L_\infty(1 - \exp(-k_2(A_{i,j}^* - t_0))) \times \left(\frac{1 + \exp(-\beta(A_{i,j}^* - t_0 - \alpha))}{1 + \exp(\beta\alpha)} \right)^{\frac{(k_1 - k_2)}{\beta}} + \varepsilon_{i,j} \quad (2)$$

where the length measurement errors $\varepsilon_{i,j}$ were assumed to be independent and normally distributed around zero with a common variance $\sigma_{\varepsilon_j}^2$.

Consider $\theta_{g1} = \{L_\infty, k_1, k_2, t_0, \alpha, \beta\}$ the vector of growth parameters, θ_a the vector of ageing parameters. Let $I_{i,j}^*$ the number of counted increments for fish i at time j , i.e. either at tagging or at recapture, $\pi[\theta_{g1}|L_{i,j}^*, A_{i,j}]$, $\pi[\theta_a|I_{i,j}^*]$, denote the posterior distributions of the parameters and $\pi[\theta_{g1}]$, $\pi[\theta_a]$, $\pi[p]$ denote their prior distributions. Here, $A_{i,j}$ are not directly observable latent variables. The full model corresponds to the joint distribution of parameters and latent variables. $L_{i,j}^*$ and $I_{i,j}^*$ being independent, this joint posterior distribution can be written as:

$$\pi[\theta_{g1}, \theta_a|L_{i,j}^*, I_{i,j}^*] \propto \pi[L_{i,j}^*, A_{i,j}|\theta_{g1}] \times \pi[I_{i,j}^*|A_{i,j}, \theta_a] \times \pi[\theta_{g1}] \times \pi[\theta_a] \quad (3)$$

where $\pi[L_{i,j}^*, A_{i,j}|\theta_{g1}]$ represents the conditional gaussian likelihood of observed lengths. Thus, the length values were predicted from the joint density:

$$f(L_j^*|I_j^*, \theta_{g1}) = \int \pi[L_{i,j}^*|A_{i,j}, \theta_{g1}] \times \pi[A_{i,j}|I_{i,j}^*, \theta_a] .dA_{i,j} \quad (4)$$

The product of the joint densities over all fish gives the likelihood function for the direct ageing data, and the negative likelihood was expressed as:

$$-ln(\mathcal{L}_1) = - \sum_i \sum_j f(L_{i,j}^*|I_{i,j}^*, \theta_{g1}) \quad (5)$$

2.2.3 Fitting to mark-recapture data

In mark-recapture data, a fish of length L_1 was tagged and released at time t_1 and then recaptured at time t_2 with length L_2 . The change in fish size over the time interval $[t_2, t_1]$ called time-at-liberty (T_L) is a monotone increasing function of time expressed as follows (Wang, 1998):

$$L(t_2) = L(t_1) + (L_\infty - L(t_1)) \times (1 - \exp(-K(t_1, t_2))) \quad \text{with} \quad K(t_1, t_2) = \int_{t_1}^{t_2} k(t) .dt \quad (6)$$

$k(t)$ is the logistic function controlling the change in growth. From this form, we can express the length L_2 as a function of L_1 and T_L for each fish i :

$$L_{i,2}^* = L_{i,1}^* + (L_\infty - L_{i,1}^*) (1 - \exp(-k_2 \times T_{Li}^*)) \times \left(\frac{1 + \exp(-\beta(t_{1i} + T_L^* - t_0 - \alpha))}{1 + \exp(-\beta(t_{1i} - t_0 - \alpha))} \right)^{\frac{(k_1 - k_2)}{\beta}} + \varepsilon_{i,2} \quad (7)$$

where t_1 refers to the age at tagging. With mark-recapture data, the absolute age of fish is unknown and therefore these data provide no information to estimate the parameters α and t_0 . We defined a new parameter λ such as for each fish i , $\lambda_i = \alpha + t_0 - t_{1i}$. λ varied from one fish to another because the fish are spawned at different times and they do not grow all at the same rate. Thus, the VB log K model (Eq. 11) for mark-recapture data had the following form:

$$L_{i,2}^* = L_{i,1}^* + (L_\infty - L_{i,1}^*) (1 - \exp(-k_2 \times T_{Li}^*)) \times \left(\frac{1 + \exp(-\beta(T_{Li}^* - \lambda_i))}{1 + \exp(\beta \times \lambda_i)} \right)^{\frac{(k_1 - k_2)}{\beta}} + \varepsilon_{i,2} \quad (8)$$

The λ_i parameters were used to relax the constraint on the anchor the growth curve which increase model flexibility. The joint posterior distribution of mark-recapture model was written as:

$$\pi[\theta_{g2}, \lambda_{ri} | L_{i,2}^*, L_{i,1}^*, T_{Li}^*] \propto \pi[L_{i,2}^*, L_{i,1}^*, T_{Li}^* | \theta_{g2}, \lambda_{ri}] \times \pi[\theta_{g2}] \times \pi[\lambda_{ri}] \quad (9)$$

where $\theta_{g2} = \{k_1, k_2, \beta\}$, and its negative likelihood as:

$$-ln(\mathcal{L}_2) = - \sum_i f(L_{i,2}^* | L_{i,1}^*, T_{Li}^*, \theta_{g2}, \lambda_{ri}) = - \sum_i \int \pi[L_{i,2}^*, L_{i,1}^*, T_{Li}^* | \theta_{g2}, \lambda_{ri}] .dL_{i,1}^* .dT_{Li}^* \quad (10)$$

2.2.4 Fitting to modal progression data

The modal progressions estimated from length-frequency distribution can be treated as multiple mark-recapture events where the initial age would be known. Let $\mu_{c,k}$ the length mode value for the cohort c , equated with a fish, at the time k , equated with the opportunity of capture, and let $a_{c,1}$

the mean age for the first mode. The time interval between two successive length modes, here one month, is denoted by d . The corresponding mean age for the length mode $\mu_{c,k}$ is $a_{c,k} = a_{c,1} + (k-1)d$. Thus, from Eq.11:

$$\mu_{c,k}^* = L_\infty(1 - \exp(-k_2(a_{c,1}^* + (k-1)d - t_0))) \times \left(\frac{1 + \exp(-\beta(a_{c,1}^* + (k-1)d - t_0 - \alpha))}{1 + \exp(\beta\alpha)} \right)^{\frac{(k_1 - k_2)}{\beta}} \times \varepsilon_{\mu_{c,k}} \quad (11)$$

where $\varepsilon_{\mu_{c,k}}$ are the uncertainty on the modal length. They were assumed to be independent and normally distributed around zero with a common variance σ_μ . Owing to a slower growth and an increase of individual variability in size-age relationship with increasing age (especially after the sexual maturity), overlaps between two successive length-at-age distributions increases and makes the identification of modes increasingly difficult. So, we considered here a multiplicative error.

The joint posterior distribution of modal progressions model was written as:

$$\pi[\theta_{g3} | \mu_{c,k}^*, a_{c,1}^*] \propto \pi[\mu_{c,k}^*, a_{c,1}^* | \theta_{g3}] \times \pi[\theta_{g3}] \quad (12)$$

where $\theta_{g3} = \{L_\infty, k_1, k_2, t_0, \alpha, \beta, \sigma_\mu\}$, and its negative likelihood as:

$$-\ln(\mathcal{L}_3) = -\sum_i f(\mu_{c,k}^* | a_{c,1}^*, \theta_{g2}) = -\sum_i \int \pi[\mu_{c,k}^*, a_{c,1}^* | \theta_{g3}] \cdot da_{c,1}^* \quad (13)$$

2.2.5 Bayesian fit of integrated growth model

The three data sources being independent, the overall negative log-likelihood is the sum of the log-likelihood defined in Eqs. 5, 10 and 13:

$$-\ln(\mathcal{L}) = -(\ln(\mathcal{L}_1) + \ln(\mathcal{L}_2) + \ln(\mathcal{L}_3)) \quad (14)$$

For the bigeye, an alternative model, without direct ageing data, was run. The integrated growth models were fitted to the data using a Bayesian inference. In a Bayesian framework, the parameters θ are treated as random variables and a prior probability distribution is their assigned (Table 3). This offers the possibility of introducing expert knowledges in the model.

The asymptotic length L_∞ , maximal length that a fish can reach, is a particularly important parameter because it determines the shape of the second part of the growth curve. Since the data set included little information on the asymptotic part of the growth curve, auxiliary information was provided for this parameter consistently with the available knowledge on the biology of the species. An informative prior distribution was defined for L_∞ through the use of a generalized extreme value distribution (GEV), which allows extrapolation of the distribution tails behavior from the greatest values of a sample and thus estimates the occurrence probability of extreme events (Borchani, 2010). The choice of this distribution is motivated by the fact that tunas grow throughout their life so that

the largest observed sizes should correspond to the oldest fish. The distribution was fitted based on size measurement data on fresh fish collected during 1952-2011 from the European and Seychelles purse seine fisheries, Maldivian pole and line vessels, and Taiwanese and Japanese longliners.

The growth rate coefficients k_1 and k_2 are in part model-specific and weakly informative priors were assigned to them. k_1 was assumed to vary according to a gamma prior distribution with mean and coefficient of variation determined from the literature. k_2 was set equal to $k_1 + \kappa$ with κ following a uniform distribution (Appendix B, Tables B.1 and B.2).

The transition rate β between k_1 and k_2 which is specific to the VB-logK model and the theoretical age of zero length t_0 that depends on the data were assigned weakly informative distributions.

The parameter α is the mean age relative to t_0 at which change in growth occurs and was assigned a weakly informative prior gamma distribution with mean defined from the literature on yellowfin growth (Gascuel et al., 1992; Lehodey and Leroy, 1999; Lumineau, 2002; Viera, 2005). For the big-eye, no prior information was available in the literature. However, this species being physiologically close to yellowfin, we have supposed that the same prior might be used.

The standard deviation of size measurement errors σ_{ε_j} was determined from fork length differences of RTTP-IO fishes released and recaptured several times with time-at-liberty less than or equal to 7 days. These individuals were not included in subsequent analyses and therefore constitute an independent data set. On the other hand, some recapture lengths were measured on frozen fish, that may include a bias due to tuna shrinkage: frozen fish in brine are often severely compressed. This shrinkage bias was estimated from some fish that have been thawed and remeasured with a good precision. But, the length could as well be overestimated or underestimated. Thus, the standard deviation values σ_{ε_j} was estimated to 3 at tagging and 5 at recapture.

The standard deviation of modal length errors σ_{μ} was unknown and an uninformative inverse gamma distribution their assigned.

λ_i are adjustment parameters and uniform distributions defined on the interval $[-5; 5]$ have been assigned.

The initial mean ages $a_{c,1}$ were estimated with a precision of 3-4 months and were distributed around the estimated age according to a gamma distribution.

Estimates of age and growth parameters were evaluated from three Markov Chain Monte Carlo (MCMC) simulations using a Gibbs sampler as implemented in OpenBugs version 3.2.1 (Spiegelhalter et al., 2011). The convergence of the MCMC to stationary posterior distribution was evaluated from the Gelman-Rubin diagnostic, based on the ratio of inter-chain variance on intra-chain variance. It must be close to 1 for getting convergence (Gelman and Rubin, 1992). Convergence is reached when the influence of the likelihood dominates the prior information resulting in indistinguishable chains outputs. This diagnostic is computed from second half of MCMC simulation samples.

Table 3: Prior distribution used for parameters of somatic growth models. All variables are defined in Table

| Yellowfin | Bigeye |
|---|---|
| $L_\infty \sim GEV(173.141, 11.067, -0.3474)$ | $L_\infty \sim GEV(187.622, 9.189, -0.3313)$ |
| $k_1 \sim \Gamma(2.778, 0.211)$ | $k_1 \sim \Gamma(4, 0.058)$ |
| $k_2 = k_1 + \kappa$ with $\kappa \sim \mathcal{U}(0, 3)$ | $k_2 = k_1 + \kappa$ with $\kappa \sim \mathcal{U}(0, 3)$ |
| $\alpha \sim \Gamma(25, 1)$ | $\alpha \sim \Gamma(25, 1)$ |
| $\beta \sim \Gamma(4, 3.5)$ | $\beta \sim \mathcal{U}(0, 30)$ |
| $t_0 \sim \mathcal{U}(-2, 0)$ | $t_0 \sim \mathcal{U}(-2, 0)$ |
| $\varepsilon_{i,j} \sim \mathcal{N}(0, \sigma_{\varepsilon_j}^2)$ with σ_{ε_j} estimated to 3 at tagging and to 5 at recapture | |
| $\varepsilon_{\mu,c,j} \sim \mathcal{N}(0, \sigma_\mu^2)$ with $\sigma_\mu \sim Inv\Gamma(0.04, 0.01)$ | |

3 Results

3.1 Model diagnostic

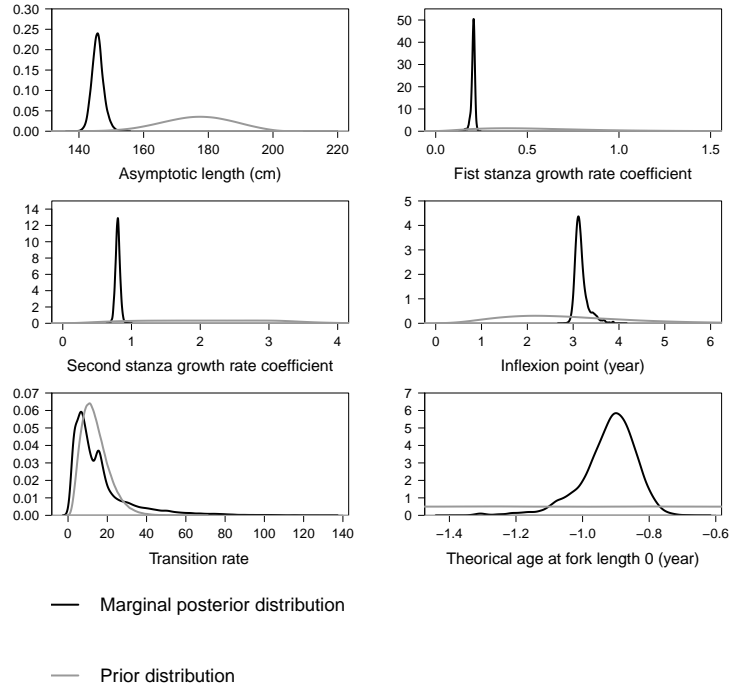


Figure 4: Marginal posterior distribution of integrated yellowfin growth model

The marginal posterior distributions were drawn from samples of three MCMC chains. A burn-in period of 5,000 iterations was initially rejected. The Gelman-Rubin diagnostic of each parameters was computed from second half of MCMC simulation samples. For the three population growth

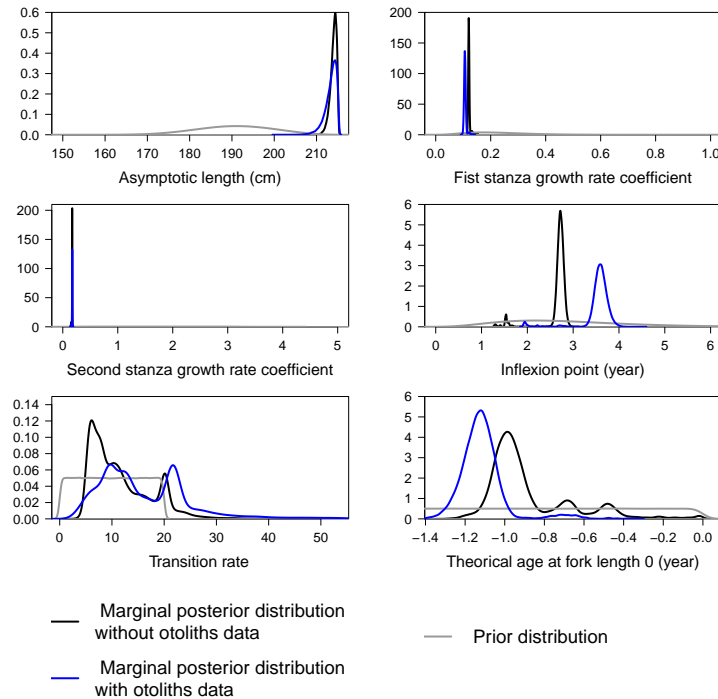


Figure 5: Marginal posterior distribution of integrated bigeye growth models

models, that for yellowfin and those for bigeye, the values were closed to 1.0, indicating convergence, with a multivariate potential scale reduction factor of 1.03 for the yellowfin model and of 1.09 and 1.07 for the bigeye model with and without otolith readings data respectively.

Checking the posterior distributions for the yellowfin model (Fig. 4) suggested a good model's ability to use the information provided by the data to estimate the parameters. With the exception of the β parameter, the posterior distributions were narrow compared to the prior distributions with a shift of distributions indicating that the data were enough informative and the priors were well-updated from the data. The marginal posterior distribution of β showed some irregularities and a high standard deviation which revealed a model difficulty in estimating this parameter most likely due to a lack of information in the data. The number of fish of known age covering the transition between the stanzas was insufficient and the mark-recapture data provided information on a average growth rate but no details to discriminate the stanzas and thus they were very little informative for estimating β . The model was sensitive to the choice of the prior for β . The use of a gamma distribution rather than an uniform distribution did not significantly modified the parameter estimates but has improved the model convergence. For the bigeye, the check of the posterior distributions (Fig. 5) revealed a good ability of the models with and without otolith readings data in estimating of L_∞ , k_1 and k_2 from the information contained in data. The posteriors of others parameters appeared irregular showing an inefficiency of the models that may result from an insufficient number of MCMC samples or from contradictory informations from otolith readings

and mark-recapture data. The integrated model with otolith readings data led to a significant underestimate of the growth over 60 cm F_L . This was due to contradictory inputs; comparatively to modal progressions, most of the otolith readings data tended to overestimate the fish ages and thus favored the lower growth rates. These otolith data included some aberrations and were considered unreliable. The model without otolith readings data led to a good fit, we have chosen to retain this last model. However, the uncertainty increased in the first part of the growth curve for the model without otolith data, meaning that these data still provided despite everything some useful informations.

The mean values and the plausible ranges for each parameter were determined from MCMC samples thinned to one draw every 1000th sample (Tables 4 and 6).

3.2 Yellowfin growth

The model supported a two-stanza growth for Indian Ocean yellowfin with 2 distinct phases over the fish lifespan (Fig. 6) characterised by 2 growth rate coefficients significantly different according to the Bayesian 95% credibility interval (Table 4). The first stanza was characterized by a relatively slow growth which gradually decreased to a minimum of 1.43 cm.month⁻¹ around 62 cm F_L at about 1.8 years. It was followed by a second stanza in which the growth accelerated up to a maximum of 4.02 cm.month⁻¹ near 81 cm F_L at about 2.46 years and then progressively decreased with size to become very slow when size was close to the asymptotic length, reaching 0.01 cm.month⁻¹ around 145 cm F_L . The mean age at which change in growth occurs was estimated about 2.25 year corresponding to a mean length of 73 cm F_L .

Fitting the model revealed significant negative correlations between the first growth rate coefficient k_1 and the mean age of growth change α (-0.84) and between the second growth rate coefficient k_2 and the asymptotic length L_∞ (-0.92; Table 5). This latter is found in most studies using a model derived from the Von Bertalanffy model as the VB log K. These correlations reflect a trade-off between growth and reproduction such as high growth rates lead to an earlier acquisition of sexual maturity resulting in a smaller asymptotic length. Likewise significant correlations negative between α and the age at zero length t_0 and positive between k_1 and t_0 were found. These correlations can result in some difficulty to estimate the posterior distribution as well as a poor parameters estimation because some possibilities for the posterior distributions may never be sampled due to prior ranges of correlated parameters. Thus, the negative correlation between k_2 and L_∞ could be, in part, the cause of the low value obtained for the asymptotic length.

The mean asymptotic length was estimated at 145.88 cm F_L , between 142.6 cm F_L and 150 cm F_L (Table 4). This value seems consistent with the dataset including very few fish over 150 cm, the largest fish having a length of 159 cm F_L . However, this value was very low comparatively to the value estimated at about 173 cm from the catch of the purse seiners and longliners used for GEV estimate and to the maximum lengths of 200 cm that have been observed for Indian Ocean yellowfin. The current growth curve reflects the growth of the exploited population, mainly by

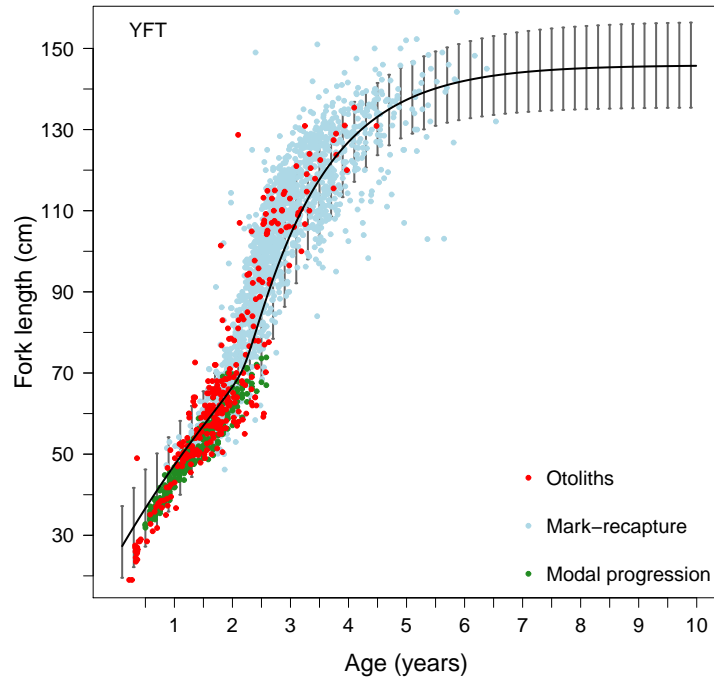


Figure 6: Yellowfin growth curve as estimated from the integrated model

Table 4: Attributes of marginal posterior distributions for yellowfin integrated growth model

| Parameters | Mode | Mean | Std. dev. | Posterior quantiles | |
|------------------------------|---------|--------|-----------|---------------------|---------|
| | | | | 2.5% | 97.5% |
| L_{∞} (cm) | 145.543 | 145.88 | 1.9 | 142.597 | 150.002 |
| α (years) | 3.104 | 3.166 | 0.14 | 2.983 | 3.533 |
| β | 6.692 | 16.653 | 14.73 | 2.436 | 58.93 |
| k_1 (years ⁻¹) | 0.207 | 0.204 | 0.01 | 0.182 | 0.22 |
| k_2 (years ⁻¹) | 0.797 | 0.799 | 0.035 | 0.729 | 0.866 |
| t_0 (years) | -0.884 | -0.919 | 0.086 | -1.117 | -0.791 |
| σ_{μ} (cm) | 0.048 | 0.049 | 0.003 | 0.044 | 0.055 |

Table 5: Correlation matrix of yellowfin growth parameters

| | α | β | k_1 | k_2 | κ | t_0 |
|--------------|----------|---------|--------|--------|----------|--------|
| L_{∞} | 0.054 | 0.064 | -0.4 | -0.924 | -0.817 | -0.107 |
| α | 1 | -0.376 | -0.841 | 0.145 | 0.415 | -0.862 |
| β | | 1 | 0.331 | -0.16 | -0.269 | 0.303 |
| k_1 | | | 1 | 0.222 | -0.09 | 0.895 |
| k_2 | | | | 1 | 0.951 | -0.036 |
| κ | | | | | 1 | -0.321 |

purse seiners for which catches fish over 150 cm are unusual, is therefore not representative of the wild population.

Besides, the mean growth curve underestimated the growth speed below 40 cm F_L . The data suggested a three-stanza growth with an initially growth more faster than expected until 40 cm. But the VB log K model is not able to take account this third stanza.

3.3 Bigeye growth

For the Indian Ocean bigeye, the model supported a two-stanza growth slightly pronounced (Fig. 7) but related to 2 growth rate coefficients significantly different according to the Bayesian 95% credibility interval (Table 6). The first stanza was characterized by a slower growth which gradually decreased to a minimum of 1.64 cm.month⁻¹ around 54 cm F_L at about 1.5 years. During the second stanza, the growth accelerated up to a maximum of 2.08 cm.month⁻¹ near 65 cm F_L at about 2 years and then progressively decreased with size. The mean age at which change in growth occurs was estimated about 1.8 year corresponding to a mean length of 60 cm F_L .

Fitting the model did appear significative negative correlations between k_1 and α (-0.79) and between k_1 and k_2 (-0.71) and a significative positive correlation between k_2 and α (0.813; Table 7). These correlations mean that a decrease in the age at maturity, due to a high initial growth rate, cause a decrease in the growth rate. This is also a trade-off between growth and reproduction.

Table 6: Attributes of marginal posterior distributions for bigeye integrated growth models

| Parameters | Without otolith readings data | | | | | With otolith readings data | | | | |
|------------------------------|-------------------------------|---------|-----------|---------------------|--------|----------------------------|---------|-----------|---------------------|-------|
| | Mode | Mean | Std. dev. | Posterior quantiles | | Mode | Mean | Std. dev. | Posterior quantiles | |
| | | | | 2.5% | 97.5% | | | | 2.5% | 97.5% |
| L_∞ (cm) | 214.273 | 213.945 | 0.799 | 211.947 | 215.1 | 214.219 | 213.456 | 1.35 | 209.695 | 215.1 |
| α (years) | 2.723 | 2.665 | 0.279 | 1.533 | 2.871 | 3.635 | 3.563 | 0.297 | 2.508 | 3.89 |
| β | 10.015 | 12.026 | 6.255 | 5.356 | 24.595 | 15.997 | 8.95 | 4.59 | 39.249 | 7.29 |
| k_1 (years ⁻¹) | 0.12 | 0.121 | 0.004 | 0.116 | 0.133 | 0.106 | 0.106 | 0.004 | 0.1 | 0.11 |
| k_2 (years ⁻¹) | 0.171 | 0.171 | 0.003 | 0.16 | 0.175 | 0.172 | 0.171 | 0.005 | 0.157 | 0.17 |
| t_0 (years) | -0.991 | -0.886 | 0.21 | -1.119 | -0.389 | -1.132 | -1.121 | 0.114 | -1.302 | -0.74 |
| σ_μ (cm) | 1.057 | 1.059 | 0.005 | 1.053 | 1.078 | 1.07 | 1.071 | 0.005 | 1.063 | 1.08 |

Table 7: Correlation matrix of bigeye growth parameters

| | α | β | k_1 | k_2 | κ | t_0 |
|------------|----------|---------|--------|--------|----------|--------|
| L_∞ | -0.087 | -0.05 | -0.055 | -0.369 | -0.14 | -0.001 |
| α | 1 | 0.036 | -0.791 | 0.813 | 0.864 | -0.638 |
| β | | 1 | -0.046 | 0.047 | 0.05 | -0.004 |
| k_1 | | | 1 | -0.713 | -0.944 | 0.664 |
| k_2 | | | | 1 | 0.904 | -0.55 |
| κ | | | | | 1 | -0.663 |

The mean asymptotic length was estimated at 213.9 cm F_L (Table 6). This value was much higher than the maximal value observed in the data, 189 cm F_L , and the mean value of GEV estimated

at 187.6 cm. But, it was close to the maximal length from the purse seiners and longliners catches of 206 cm and it seemed consistent with the knowledge of the species. Although the catches of individuals above 180 cm are unusual, the larger individuals can reach 200 cm F_L in Indian Ocean (IOTC 2011) and until 250 cm in Atlantic Ocean (Riener, 1996). However, according to the mean growth curve, bigeye could reach this asymptotic size after a thirty years, which is much higher than the life expectancy of this species around 15 years (IOTC 2011).

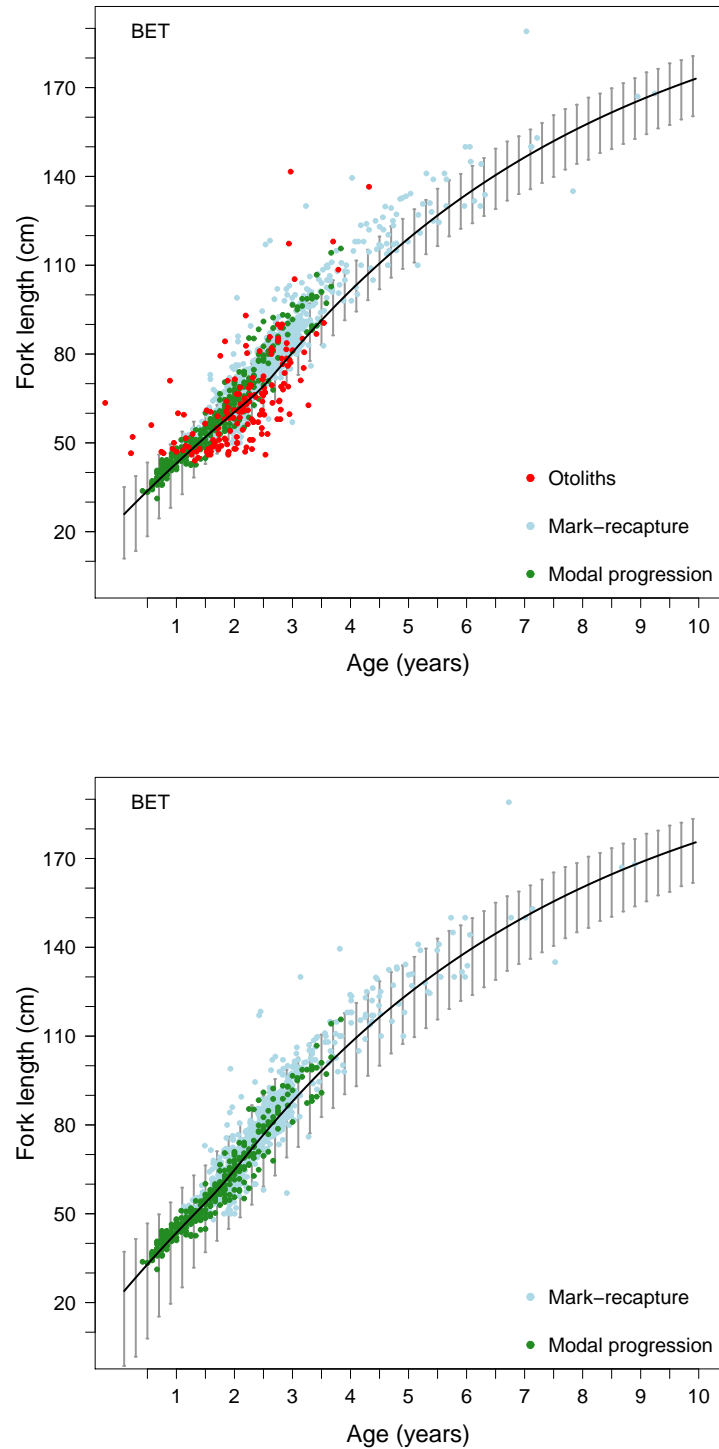


Figure 7: Bigeye growth curve as estimated from the integrated models with and without otolith readings data

References

- Borchani, A. (2010). Statistiques des valeurs extrêmes dans le cas de lois discrètes. Technical Report ESSEC Working Paper 10009, ESSEC Business School.
- Chantawong, P., Panjarat, S., and Singtongyam, W. (1999). Preliminary results on fisheries and biology of bigeye tuna (*Thunnus obesus*) in the eastern Indian Ocean. *IOTC Proceedings*, 12(2):231–241.
- Chen, Y., Jiao, Y., and Chen, L. (2003). Developing robust frequentist and Bayesian fish stock assessment methods. *Fish and Fisheries*, 4:105–120.
- Clark, J. S. (2005). Why environmental scientists are becoming Bayesians. *Ecology Letters*, 8(1):2–14.
- Cressie, N., Calder, C., Clark, J., Ver Hoef, J., and Wikle, C. (2009). Accounting for uncertainty in ecological analysis: the strengths and limitations of hierarchical statistical modeling. *Ecological Applications*, 19(3):553–570.
- Dortel, E., Massiot-Granier, F., Rivot, E., Million, J., Hallier, J., Morize, E., Munaron, J., Bousquet, N., and Chassot, E. (in prep.). Accounting for age uncertainty in growth modeling, the case study of yellowfin tuna (*Thunnus albacares*) of the Indian Ocean.
- Eveson, J. and Million, J. (2008). Estimation of growth parameters for yellowfin, bigeye and skipjack tuna using tag-recapture data. *IOTC-Working Party on Tagging Data Analysis*, 7(07):31p.
- Eveson, J. P., Laslett, G. M., and Polacheck, T. (2004). An integrated model for growth incorporating tag-recapture, length-frequency, and direct aging data. *Canadian Journal of Aquatic and Fisheries Sciences*, 61:292–306.
- Fonteneau, A. and Gascuel, D. (2008). Growth rates and apparent growth curves, for yellowfin, skipjack and bigeye tagged and recovered in the Indian Ocean during the IOTTP. *IOTC-WPTDA*, 8:23p.
- Gascuel, D., Fonteneau, A., and Capisano, C. (1992). Modélisation d’une croissance en deux stances chez l’albacore (*Thunnus albacares*) de l’Atlantique Est. *Aquatic Living Resources*, 5:155–172.
- Gelman, A., Carlin, J., Stern, H., and Rubin, D. (2004). *Bayesian Data Analysis, Second Edition*. Chapman & Hall/CRC Texts in Statistical Science, CRC press book edition.
- Gelman, A. and Rubin, D. (1992). Inference from iterative simulation using multiple sequences. *Statistical Science*, 7(4):457–511.
- Hallier, J. (2008). Status of the Indian Ocean tuna tagging programme - RTTP-IO. *IOTC-WPTDA*, 10:40p.

- Hasselblad, V. (1966). Estimation of parameters for a mixture of normal distributions. *Technometrics*, 8(3):431–444.
- Helser, T. and Lai, H.-L. (2004). A Bayesian hierarchical meta-analysis of fish growth: with an example for North American largemouth bass, *Micropterus salmoides*. *Ecological Modelling*, 178:399–416.
- Herrera, M. and Pierre, L. (2010). Status of IOTC databases for tropical tunas. *IOTC-WPTT*, 3:28p.
- Kume, S. and Joseph, J. (1966). Size composition, growth and sexual maturity of bigeye tuna, *Thunnus obesus* (Lowe), from the Japanese long-line fishery in the Eastern Pacific Ocean. *Inter-American Tropical Tuna Commission Bulletin*, 11(2):47–75.
- Langley, A., Herrera, M., and Million, J. (2010). Stock assessment of yellowfin tuna in the Indian Ocean using MULTIFAN-CL. *IOTC-WPTT*, 23:72p.
- Laslett, G., Eveson, J., and Polacheck, T. (2002). A flexible maximum likelihood approach for fitting growth curves to tag-recapture data. *Canadian Journal of Fisheries and Aquatic Sciences*, 59:976–986.
- Le Guen, J. and Sakagawa, G. (1973). Apparent growth of yellowfin tuna from the Eastern Atlantic ocean. *Fishery Bulletin*, 71(1):175–187.
- Lehodey, P. and Leroy, B. (1999). Age and growth of yellowfin tuna (*Thunnus albacares*) from the western and central Pacific Ocean as indicated by daily growth increments and tagging data. *12th Meeting of the SCTB, Working Paper YFT-2*, pages 1–21.
- Lumineau, O. (2002). Study of the growth of Yellowfin tuna (*Thunnus albacares*) in the Western Indian Ocean based on length frequency data. *IOTC Proceedings*, 5:316–327.
- Macdonald, P. and Green, P. (1988). User's guide to program MIX: An interactive program for fitting mixtures of distributions. *Ichthus Data Systems*.
- Marriott, R. J. and Mapstone, B. D. (2006). Consequences of inappropriate criteria for accepting age estimates from otoliths, with a case study for a long-lived tropical reef fish. *Canadian Journal of Fisheries and Aquatic Sciences*, 63(10):2259–2274.
- Marsac, F. (1991). Preliminary study of the growth of yellowfin estimated from purse seine data in the Western Indian Ocean. *IPTP Collective volume of working documents*, 6:35–39.
- Marsac, F. and Lablache, G. (1985). Preliminary study of the growth of yellowfin estimated from purse seine data in the Western Indian Ocean. *IPTP Collective volume of working documents*, pages 91–110.

- McAllister, M., Pikitch, E., and Babcock, E. (2001). Using demographic methods to construct Bayesian priors for the intrinsic rate of increase in the Schaefer model and implications for stock rebuilding. *Canadian Journal of Fisheries and Aquatic Sciences*, 58:1871–1890.
- Morize, E., Munaron, J.-M., Hallier, J.-P., and Million, J. (2008). Preliminary growth studies of yellowfin and bigeye tuna (*Thunnus albacares* and *T. obesus*) in the Indian Ocean by otolith analysis. pages 1–13.
- Neilson, J. (1992). Sources of error in otolith microstructure examination In D.K. Stevenson and S.E. Campana, Otolith microstructure examination and analysis. *Canadian Special Publication Fisheries Aquatic Science*, 117:115–126.
- Nootmorn, P. (2004). Reproductive biology of bigeye tuna in the Eastern Indian Ocean. *IOTC Proceedings*, 7:1–5.
- Nootmorn, P., Yakoh, A., and Kawises, K. (2005). Reproductive biology of yellowfin tuna in the Eastern Indian Ocean. *IOTC-WPTT*, 14:379–385.
- Panfili, J., De Pontual, H., Troadec, H., and Wright, P. (2002). *Manuel de sclérochronologie des poissons*. Coédition Ifremer-IRD.
- Panfili, J., Tomas, J., and Morales-Nin, B. (2009). Otolith microstructure in tropical fish. In *Tropical fish otoliths: information for assessment, management and ecology*, Methods and Technologies in Fish Biology and Fisheries Volume 11: 212-248. Green B.S. et al. [Ed.].
- Punt, A. and Hilborn, R. (1997). Fisheries stock assessment and decision analysis: the Bayesian approach. *Reviews in Fish Biology and Fisheries*, 7:35–63.
- Radtke, R. and Fey, D. P. (1996). Environmental effects on primary increment formation in the otoliths of newly-hatched Arctic charr. *Journal of Fish Biology*, 48(6):1238–1255.
- Restrepo, V., Diaz, G., Walter, J., Neilson, J., Campana, S., Secor, D., and Wingate, R. (2010). Updated estimate of the growth curve of Western Atlantic bluefin tuna. *Aquatic Living Resources*, 23:335–342.
- Riener, F. (1996). Catálogo dos peixes do Arquipélago de Cabo Verde. *Publicações avulsas do IPIMAR*, (2):339.
- Romanov, E. and Korotkova, L. (1988). Age and growth rates of yellowfin tuna *Thunnus albacares* (Bonnaterre 1788) (Pisces, Scombridae) in the north-western part of the Indian Ocean, determined by counting the rings of vertebrae. *FAO/IPTP Collection Volume of Working Documents*, 3:68–73.
- Schnute, J. and Fournier, D. (1980). A new approach to length-frequency analysis: growth structure. *Canadian Journal of Fisheries and Aquatic Sciences*, 37(9).

- Secor, D., Dean, J., and Laban, E. (1991). Manual for otolith removal and preparation for microstructural examination. *Electric Power Research Institute and the Belle W. Baruch Institute for Marine Biology and Coastal Research*.
- Spiegelhalter, D., Thomas, A., Best, N., and Lunn, D. (2011). OpenBUGS version 3.2.1 user manual.
- Stéquert, B. (1995). Détermination de l'âge des thons tropicaux à partir de leurs otolithes: exemple du Yellowfin (*Thunnus albacares*). *Document Technique du Centre ORSTOM de Brest*, 76:1–31.
- Stéquert, B. and Conand, F. (2004). Age and growth of bigeye tuna (*Thunnus obesus*) in the Western Indian Ocean. *Cybium*, 28(2):163–170.
- Stéquert, B., Rodriguez, J., Cuisset, B., and Le Menn, F. (2001). Gonadosomatic index and seasonal variations of plasma sex steroids in skipjack tuna (*Katsuwonus pelamis*) and yellowfin tuna (*Thunnus albacares*) from the Western Indian Ocean. *Aquatic Living Resources*, 14:313–318.
- Uchiyama, J. and Struhsaker, P. (1981). Age and growth of skipjack tuna, *Katsuwonus pelamis*, and yellowfin tuna, *Thunnus albacares* as indicated by daily growth increments of sagittae. *Fishery Bulletin*, 79:151–162.
- Viera, A. (2005). Study of the growth of Yellowfin tuna (*Thunnus albacares*) in the Indian Ocean based on length-frequency data from 2000 to 2004. *IOTC-WPTT*, 32:17p.
- Wang, Y.-G. (1998). Growth curves with explanatory variables and estimation of the effect of tagging. *Australian and New Zealand Journal of Statistics*, 40(3):299–304.
- Wild, A. (1986). Growth of yellowfin tuna, *Thunnus albacares*, in the Eastern Pacific Ocean based on otolith increments. *Inter-American Tropical Tuna Commission Bulletin*, 18(6):423–479.
- Wild, A. and Foreman, T. (1980). The relationship between otolith increments and time for yellowfin and skipjack tuna marked with tetracycline. *Inter-American Tropical Tuna Commission Bulletin*, 17(7):507–560.
- Wild, A., Wexler, J., and Foreman, T. (1995). Extended studies of increment deposition rates in otoliths of yellowfin and skipjack tunas. *Bulletin of Marine Science*, 57(2):555–562.
- Zhu, G., Xu, L., Zhou, Y., and Song, L. (2008). Reproductive Biology of Yellowfin Tuna *T. albacares* in the West-Central Indian Ocean. *Journal of Ocean University of China*, 7(3):327–332.
- Zudaire, I., Murua, H., Grande, M., Korta, M., Arrizabalaga, H., Areso, J., and Delgado-Molina, A. (2010). Reproductive biology of yellowfin tuna (*Thunnus albacares*) in the Western and Central Indian Ocean. *IOTC-WPTT*, 48:25p.

4 Supplemental material

Appendix A: Ageing error model

1 Model description

A hierarchical model that explicitly accounts for process and interpretation errors in otolith readings was developed to estimate the age of each fish. The stochastic processes associated with otolith preparation and reading were modelled through the choice of an error structure and elicitation of informative prior density functions based on expert judgment (Tables A.1 and A.2). In a first step, the hypothesis of daily increment deposition in otoliths, that has been observed for the eastern Pacific yellowfin tuna (Wild and Foreman, 1980; Wild et al., 1995), was tested based on a subset of data of OTC-tagged otoliths. The information on the process of increment deposition was subsequently used for estimating the age of yellowfin based on counts of otolith increments.

Modeling observation errors: Otoliths of each tuna species, yellowfin and bigeye, have been read by two teams. The divergences between the teams came from reading method applied and from readers experience. There were three teams, 1 and 2 for yellowfin and 2 and 3 for bigeye. For a given readers team, we assumed that the discrepancies between repeated readings of the same otolith mainly resulted from errors in interpreting missing increments and, to a lesser extent, from errors in counting, i.e. increment omission or multiple counts. The counting errors were considered to be equiprobable. Each increment has the same independent probability of misinterpretation, so errors tend to increase with age. In addition, the identification and interpretation of increments become increasingly difficult with increasing distance from the nucleus. Thereby, the relative reading error was considered to be dependent on the fish true age and a multiplicative error was used. The relative percentage of misread increments for the readers team r p_r was a constant factor assumed to be uniformly distributed between 0 and 0.5 (Table A.2, Eq. P4). For each reading of the same otolith, the reader was assumed to have the same probability of underestimating or overestimating the number of increments. The number of increments counted for reading l of otolith i ($I_{i,l}^*$) was assumed to be distributed around the expected number of increments according to a Poisson process. Here, a normal distribution was chosen for more flexibility in modeling uncertainty in readings and since the normal distribution approximates well the Poisson distribution for large values of the Poisson parameter according to the central limit theorem (Table A.2, Eq. S1-S3).

The identification of the first growth increment is an important step to define the ageing starting point and accurately estimate fish age. The otolith nucleus is an opaque spot formed during embryonic development. The first increment is formed at hatching and appears like a discontinuity in the otolith surrounding the nucleus (Panfili et al., 2009). During preparation, excessive sanding of the otolith can result in the "disappearance" of the nucleus as well as the removal of some increments. Technical experts considered that up to 15 of the first otolith increments may be lost during preparation. These increments are then estimated with a bias of 2-3 increments (ψ_n , Table A.2, Eq. P2).

Similarly to the first increment, the marginal increment can sometimes be difficult to distinguish, the edge being an otolith part often more difficult to read because the increments near the edge are narrower and can appear laterally compressed or disappear (Neilson, 1992). In addition, the otolith must be cut perpendicularly to the daily growth axis passing by the nucleus. Here, technical experts considered that up to 20 increments might be lost at otolith edge and a estimation bias of 3-4 increments can occur (ψ_e , Table A.2, Eq. P3).

Hypothesis of daily increment deposit: In a first step, the otolith increment counts after the OTC mark (I_m) were modelled as a function of the time-at-liberty (T_L), number of days between tagging and recapture, to estimate the reading accuracy of different teams. This step was based on a subsample of OTC-tagged fishes selected for good reliability, i.e. individuals for which the date of recapture was known accurately and for which the coefficient of variation of the different readings of a given otolith was inferior or equal to 10% (Marriott and Mapstone, 2006). A Bayesian linear regression model was fitted to the data to estimate the rate of increment deposition (R) and error at the otolith edge (ψ_e) (Table A.2, Eq. S1 and D1). Under the hypothesis of a daily increment deposit, the number of increment I_m must be equal to T_L . The divergence between the estimated rate of increment deposition and its theoretical value of 1 measured the reading method's reliability. Such divergence could result from the presence of sub-daily increments interpreted as daily increments by the readers or a poor estimate of lost increments. A specific regression model was run for each readers team. We used a dilated beta distribution as prior for R so as to provide information on the limit values without particular trend in the distribution shape. Based on expert knowledge, an informative prior was considered for the marginal error ψ_e (Table A.2, Eq. P3).

Estimating age from multiple readings: In a second step, the uncertainty around multiple otolith readings was modelled to estimate the actual number of increments for each fish otolith. This increment number was then converted to age by taking into account the rate of increment deposition (R). When the date of recapture was known with precision ($CV \leq 5\%$), the age-at-tagging (At) was derived from the number of increments between the nucleus and OTC mark (It) and the age-at-recapture (Ar) was deduced from It and the time-at-liberty in order to decrease the uncertainty provided by the readings (Table A.2, Eq. D2 and D3). When the number of increments at tagging was unknown, the age at recapture was derived from the total number of increments (Ir) and the age at tagging by subtracting the time-at-liberty to this number of increments (Table A.2 Eq. D4 and D5). For the yellowfin collected through the WSTTP and those from the IOT cannery, only the age-at-recapture was estimated from the total number of increments (It). To account for uncertainty around recapture date, the time-at-liberty T_L was considered as a random variable distributed according to a uniform distribution between its minimal and maximal value. The posterior distributions of R and ψ_e estimated in the previous step for each readers team were used for estimating fish age and an informative prior was considered for the nucleus bias ψ_n . In

absence of information in the data, these distributions were not updated through the estimation.

Table A.1: Parameters and variables used in the ageing error models

| Variable | Definition |
|--------------|---|
| T_{Li} | Number of days between tagging and recapture for fish i (days) |
| At_i | Age-at-tagging for fish i (days) |
| Ar_i | Age-at-recapture for fish i (days) |
| Im_i | Number of increments between OTC mark and edge for otolith of fish i |
| $Im_{i,l}^*$ | Number of increments counted between OTC mark and edge for reading l of otolith for fish i |
| It_i | Number of increments between nucleus and OTC mark for otolith of fish i |
| $It_{i,l}^*$ | Number of increments counted between nucleus and OTC mark for reading l of otolith for fish i |
| Ir_i | Total number of increments for otolith of fish i |
| $Ir_{i,l}^*$ | Total number of increments counted for reading l of otolith for fish i |
| R_r | Ratio between number of increments after OTC mark and time-at-liberty for readers team r |
| ψ_n | Bias at the nucleus |
| ψ_{er} | Bias at otolith edge for readers team r |
| p_r | Relative percentage of misread otolith increments for readers team r |

Table A.2: Deterministic and stochastic processes used in the ageing error. All variables are defined in table A.1

| Process functions | |
|--|------|
| $Im_i = R_r \times T_{Li} - \psi_{er}$ | (D1) |
| $It_i = R_r \times At_i - \psi_n$ | (D2) |
| $Ar_i = At_i + T_{Li}$ | (D3) |
| $Ir_i = R_r \times Ar_i - \psi_n - \psi_{er}$ | (D4) |
| $At_i = Ar_i - T_{Li}$ | (D5) |
| Observation functions | |
| $Im_{i,l}^* \sim \mathcal{N}(Im_i, (p_r \times Im_i)^2)$ | (S1) |
| $It_{i,l}^* \sim \mathcal{N}(It_i, (p_r \times It_i)^2)$ | (S2) |
| $Ir_{i,l}^* \sim \mathcal{N}(Ir_i, (p_r \times Ir_i)^2)$ | (S3) |
| Prior probability distributions | |
| $R_r = 2 \times R - r'; R'_r \sim \text{Beta}(1, 1)$ | (P1) |
| $\psi_n \sim \mathcal{N}(0, 3^2)$ | (P2) |
| $\psi_{er} \sim \mathcal{N}(0, 4^2)$ | (P3) |
| $p_r \sim \mathcal{U}(0, 0.5)$ | (P4) |

2 Testing influence of reading method on growth estimate

The ageing error model was coupled to the somatic VB logK growth model (section 2.2.2) so as to estimate the growth curves from the otolith readings of each team. The models were fitted to the data using Bayesian inference (section 2.2.5).

3 Respect of daily increment deposition hypothesis

For both tuna species, the relationship between the increment counts after the OTC mark (I_m) and the time-at-liberty (T_L) depended on the readers team considered (Fig. A.1). For yellowfin, the increment deposit was underestimated for the team 1 with a mean value of 0.924, while it was overestimated for the team 2 with a mean value of 1.077. In these two case, the value of 1 was not included in the 95% Bayesian credibility interval which resulted in a significant failure of the hypothesis of daily increment deposition (Table A.3).

For bigeye, the increment deposit was underestimated by the two teams with mean values of 0.992 and 0.956 for the teams 2 and 3 respectively. According to the 95% Bayesian credibility interval, the periodicity of the deposit was significantly different from one day for the team 3 but not for the team 2 (Table A.4).

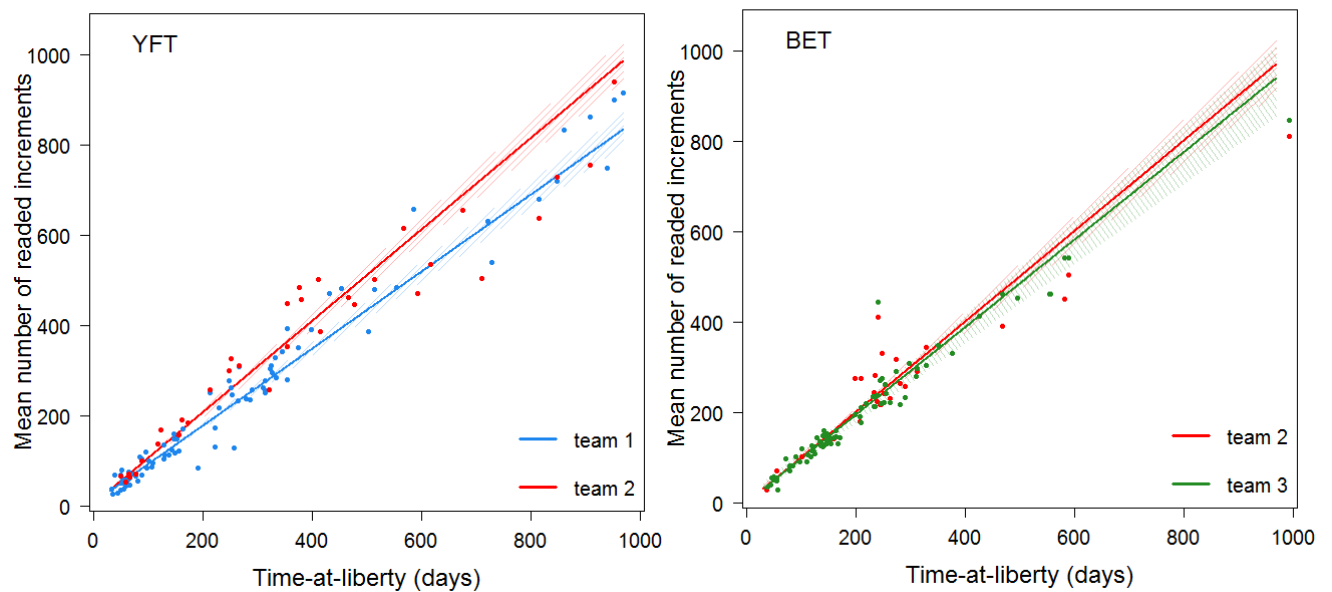


Figure A.1: Relationship between the number of increments after the OTC mark and the time-at-liberty according to the different readers teams for yellowfin (YFT) and bigeye (BET)

4 Testing influence of reading method on growth estimate

The divergences in age estimates between the readers teams had significant repercussions on the estimates of growth parameters (Fig. A.2). Thus, for yellowfin, the team 2 tended to overestimate fish ages comparatively to the team 1 and led to a much slower growth than this estimated by the team 1 (Table A.3). For bigeye, age estimates close for the two teams led to similar growth curve up to 80 cm, then the growth estimated by the team 2 was faster than this of team 3. However, there were very few data in this part of curve (Table A.4).

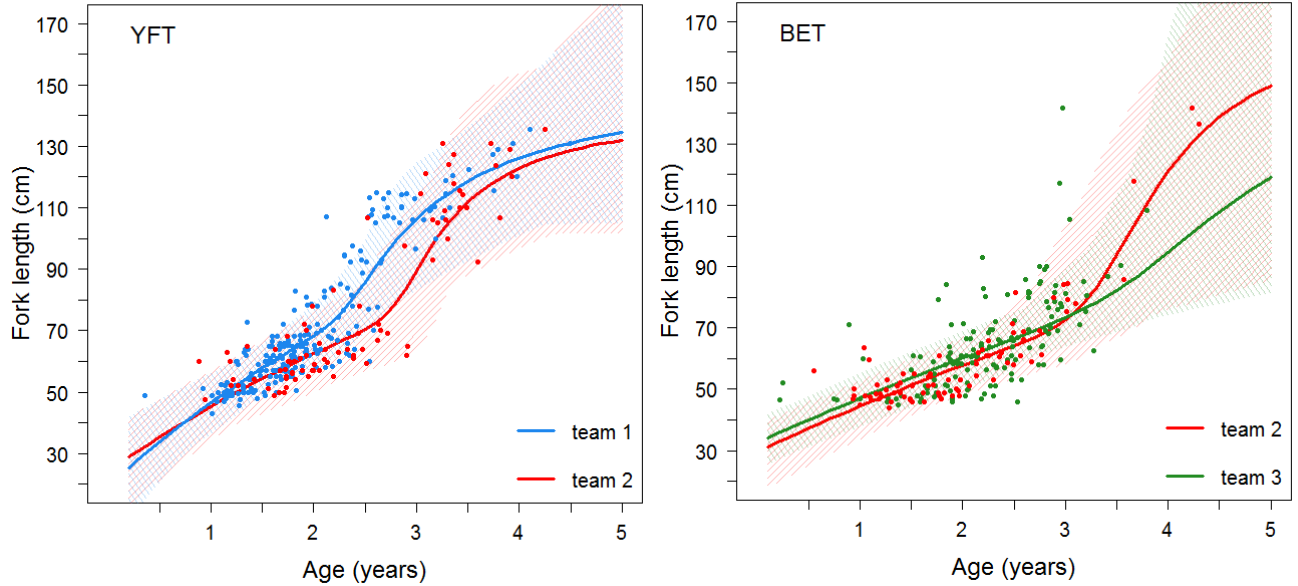


Figure A.2: Growth curves estimated from ageing data of each readers teams for yellowfin (YFT) and bigeye (BET)

Table A.3: Attributes of marginal posterior distributions for yellowfin coupled models

| Parameters | team 1 | | | | | team 2 | | | | |
|------------------------------|---------|---------|-----------|---------------------|---------|---------|---------|-----------|---------------------|---------|
| | Mode | Mean | Std. dev. | Posterior quantiles | | Mode | Mean | Std. dev. | Posterior quantiles | |
| | | | | 2.5% | 97.5% | | | | 2.5% | 97.5% |
| R_r (days) | 0.924 | 0.928 | 0.021 | 0.887 | 0.97 | 1.077 | 1.076 | 0.026 | 1.026 | 1.126 |
| ψ_{er} | -3.388 | -3.532 | 1.912 | -7.18 | 0.229 | -2.713 | -3.015 | 2.39 | -7.633 | 1.295 |
| p_r | 0.119 | 0.12 | 0.005 | 0.111 | 0.131 | 0.127 | 0.126 | 0.006 | 0.115 | 0.137 |
| L_∞ (cm) | 132.649 | 142.956 | 18.272 | 116.652 | 189.327 | 128.786 | 138.436 | 19.234 | 112.702 | 189.632 |
| α (years) | 2.843 | 2.948 | 0.442 | 2.542 | 3.812 | 3.695 | 3.787 | 0.343 | 3.198 | 4.565 |
| β | 10.243 | 15.461 | 7.92 | 2.484 | 29.322 | 16.541 | 17.364 | 7.614 | 3.842 | 29.613 |
| k_1 (years ⁻¹) | 0.249 | 0.256 | 0.055 | 0.156 | 0.374 | 0.203 | 0.212 | 0.05 | 0.119 | 0.316 |
| k_2 (years ⁻¹) | 0.745 | 1.218 | 0.704 | 0.398 | 3.036 | 1.043 | 1.681 | 0.792 | 0.466 | 3.148 |
| t_0 (years) | -0.578 | -0.603 | 0.195 | -1.065 | -0.262 | -0.908 | -0.977 | 0.313 | -1.711 | -0.455 |

Table A.4: Attributes of marginal posterior distributions for bigeye coupled models

| Parameters | team 2 | | | | | team 3 | | | | |
|------------------------------|---------|--------|-----------|---------------------|---------|---------|---------|-----------|---------------------|---------|
| | Mode | Mean | Std. dev. | Posterior quantiles | | Mode | Mean | Std. dev. | Posterior quantiles | |
| | | | | 2.5% | 97.5% | | | | 2.5% | 97.5% |
| R_r (days) | 0.992 | 0.993 | 0.025 | 0.944 | 1.041 | 0.956 | 0.955 | 0.015 | 0.926 | 0.984 |
| ψ_{er} | 0.925 | 0.736 | 2.451 | -4.478 | 5.343 | -1.4 | -1.421 | 1.489 | -4.498 | 1.366 |
| p_r | 0.14 | 0.142 | 0.009 | 0.126 | 0.16 | 0.088 | 0.088 | 0.005 | 0.078 | 0.1 |
| L_∞ (cm) | 170.096 | 171.67 | 18.781 | 136.597 | 209.002 | 180.014 | 178.735 | 18.708 | 138.868 | 208.257 |
| α (years) | 5.034 | 4.859 | 1.009 | 1.028 | 5.915 | 5.158 | 6.731 | 2.383 | 4.102 | 13.245 |
| β | 8.279 | 14.959 | 8.326 | 2.882 | 28.921 | 5.644 | 12.675 | 8.438 | 1.344 | 28.774 |
| k_1 (years ⁻¹) | 0.104 | 0.111 | 0.021 | 0.082 | 0.154 | 0.1 | 0.106 | 0.016 | 0.086 | 0.145 |
| k_2 (years ⁻¹) | 0.803 | 1.257 | 0.755 | 0.108 | 2.989 | 0.407 | 1.151 | 0.886 | 0.138 | 2.963 |
| t_0 (years) | -1.907 | -1.744 | 0.219 | -1.992 | -1.17 | -1.976 | -1.925 | 0.07 | -1.999 | -1.734 |

References

- Borchani, A. (2010). Statistiques des valeurs extrêmes dans le cas de lois discrètes. Technical Report ESSEC Working Paper 10009, ESSEC Business School.
- Chantawong, P., Panjarat, S., and Singtongyam, W. (1999). Preliminary results on fisheries and biology of bigeye tuna (*Thunnus obesus*) in the eastern Indian Ocean. *IOTC Proceedings*, 12(2):231–241.
- Chen, Y., Jiao, Y., and Chen, L. (2003). Developing robust frequentist and Bayesian fish stock assessment methods. *Fish and Fisheries*, 4:105–120.
- Clark, J. S. (2005). Why environmental scientists are becoming Bayesians. *Ecology Letters*, 8(1):2–14.
- Cressie, N., Calder, C., Clark, J., Ver Hoef, J., and Wikle, C. (2009). Accounting for uncertainty in ecological analysis: the strengths and limitations of hierarchical statistical modeling. *Ecological Applications*, 19(3):553–570.
- Dortel, E., Massiot-Granier, F., Rivot, E., Million, J., Hallier, J., Morize, E., Munaron, J., Bousquet, N., and Chassot, E. (in prep.). Accounting for age uncertainty in growth modeling, the case study of yellowfin tuna (*Thunnus albacares*) of the Indian Ocean.
- Eveson, J. and Million, J. (2008). Estimation of growth parameters for yellowfin, bigeye and skipjack tuna using tag-recapture data. *IOTC-Working Party on Tagging Data Analysis*, 7(07):31p.
- Eveson, J. P., Laslett, G. M., and Polacheck, T. (2004). An integrated model for growth incorporating tag-recapture, length-frequency, and direct aging data. *Canadian Journal of Aquatic and Fisheries Sciences*, 61:292–306.

- Fonteneau, A. and Gascuel, D. (2008). Growth rates and apparent growth curves, for yellowfin, skipjack and bigeye tagged and recovered in the Indian Ocean during the IOTTP. *IOTC-WPTDA*, 8:23p.
- Gascuel, D., Fonteneau, A., and Capisano, C. (1992). Modélisation d'une croissance en deux stances chez l'albacore (*Thunnus albacares*) de l'Atlantique Est. *Aquatic Living Resources*, 5:155–172.
- Gelman, A., Carlin, J., Stern, H., and Rubin, D. (2004). *Bayesian Data Analysis, Second Edition*. Chapman & Hall/CRC Texts in Statistical Science, CRC press book edition.
- Gelman, A. and Rubin, D. (1992). Inference from iterative simulation using multiple sequences. *Statistical Science*, 7(4):457–511.
- Hallier, J. (2008). Status of the Indian Ocean tuna tagging programme - RTTP-IO. *IOTC-WPTDA*, 10:40p.
- Hasselblad, V. (1966). Estimation of parameters for a mixture of normal distributions. *Technometrics*, 8(3):431–444.
- Helser, T. and Lai, H.-L. (2004). A Bayesian hierarchical meta-analysis of fish growth: with an example for North American largemouth bass, *Micropterus salmoides*. *Ecological Modelling*, 178:399–416.
- Herrera, M. and Pierre, L. (2010). Status of IOTC databases for tropical tunas. *IOTC-WPTT*, 3:28p.
- Kume, S. and Joseph, J. (1966). Size composition, growth and sexual maturity of bigeye tuna, *Thunnus obesus* (Lowe), from the Japanese long-line fishery in the Eastern Pacific Ocean. *Inter-American Tropical Tuna Commission Bulletin*, 11(2):47–75.
- Langley, A., Herrera, M., and Million, J. (2010). Stock assessment of yellowfin tuna in the Indian Ocean using MULTIFAN-CL. *IOTC-WPTT*, 23:72p.
- Laslett, G., Eveson, J., and Polacheck, T. (2002). A flexible maximum likelihood approach for fitting growth curves to tag-recapture data. *Canadian Journal of Fisheries and Aquatic Sciences*, 59:976–986.
- Le Guen, J. and Sakagawa, G. (1973). Apparent growth of yellowfin tuna from the Eastern Atlantic ocean. *Fishery Bulletin*, 71(1):175–187.
- Lehodey, P. and Leroy, B. (1999). Age and growth of yellowfin tuna (*Thunnus albacares*) from the western and central Pacific Ocean as indicated by daily growth increments and tagging data. *12th Meeting of the SCTB, Working Paper YFT-2*, pages 1–21.

- Lumineau, O. (2002). Study of the growth of Yellowfin tuna (*Thunnus albacares*) in the Western Indian Ocean based on length frequency data. *IOTC Proceedings*, 5:316–327.
- Macdonald, P. and Green, P. (1988). User's guide to program MIX: An interactive program for fitting mixtures of distributions. *Ichthus Data Systems*.
- Marriott, R. J. and Mapstone, B. D. (2006). Consequences of inappropriate criteria for accepting age estimates from otoliths, with a case study for a long-lived tropical reef fish. *Canadian Journal of Fisheries and Aquatic Sciences*, 63(10):2259–2274.
- Marsac, F. (1991). Preliminary study of the growth of yellowfin estimated from purse seine data in the Western Indian Ocean. *IPTP Collective volume of working documents*, 6:35–39.
- Marsac, F. and Lablache, G. (1985). Preliminary study of the growth of yellowfin estimated from purse seine data in the Western Indian Ocean. *IPTP Collective volume of working documents*, pages 91–110.
- McAllister, M., Pikitch, E., and Babcock, E. (2001). Using demographic methods to construct Bayesian priors for the intrinsic rate of increase in the Schaefer model and implications for stock rebuilding. *Canadian Journal of Fisheries and Aquatic Sciences*, 58:1871–1890.
- Morize, E., Munaron, J.-M., Hallier, J.-P., and Million, J. (2008). Preliminary growth studies of yellowfin and bigeye tuna (*Thunnus albacares* and *T. obesus*) in the Indian Ocean by otolith analysis. pages 1–13.
- Neilson, J. (1992). Sources of error in otolith microstructure examination In D.K. Stevenson and S.E. Campana, Otolith microstructure examination and analysis. *Canadian Special Publication Fisheries Aquatic Science*, 117:115–126.
- Nootmorn, P. (2004). Reproductive biology of bigeye tuna in the Eastern Indian Ocean. *IOTC Proceedings*, 7:1–5.
- Nootmorn, P., Yakoh, A., and Kawises, K. (2005). Reproductive biology of yellowfin tuna in the Eastern Indian Ocean. *IOTC-WPTT*, 14:379–385.
- Panfili, J., De Pontual, H., Troadec, H., and Wright, P. (2002). *Manuel de sclérochronologie des poissons*. Coédition Ifremer-IRD.
- Panfili, J., Tomas, J., and Morales-Nin, B. (2009). Otolith microstructure in tropical fish. In *Tropical fish otoliths: information for assessment, management and ecology*, Methods and Technologies in Fish Biology and Fisheries Volume 11: 212-248. Green B.S. et al. [Ed.].
- Punt, A. and Hilborn, R. (1997). Fisheries stock assessment and decision analysis: the Bayesian approach. *Reviews in Fish Biology and Fisheries*, 7:35–63.

- Radtke, R. and Fey, D. P. (1996). Environmental effects on primary increment formation in the otoliths of newly-hatched Arctic charr. *Journal of Fish Biology*, 48(6):1238–1255.
- Restrepo, V., Diaz, G., Walter, J., Neilson, J., Campana, S., Secor, D., and Wingate, R. (2010). Updated estimate of the growth curve of Western Atlantic bluefin tuna. *Aquatic Living Resources*, 23:335–342.
- Riener, F. (1996). Catálogo dos peixes do Arquipélago de Cabo Verde. *Publicações avulsas do IPIMAR*, (2):339.
- Romanov, E. and Korotkova, L. (1988). Age and growth rates of yellowfin tuna *Thunnus albacares* (Bonnaterre 1788) (Pisces, Scombridae) in the north-western part of the Indian Ocean, determined by counting the rings of vertebrae. *FAO/IPTP Collection Volume of Working Documents*, 3:68–73.
- Schnute, J. and Fournier, D. (1980). A new approach to length-frequency analysis: growth structure. *Canadian Journal of Fisheries and Aquatic Sciences*, 37(9).
- Secor, D., Dean, J., and Laban, E. (1991). Manual for otolith removal and preparation for microstructural examination. *Electric Power Research Institute and the Belle W. Baruch Institute for Marine Biology and Coastal Research*.
- Spiegelhalter, D., Thomas, A., Best, N., and Lunn, D. (2011). OpenBUGS version 3.2.1 user manual.
- Stéquert, B. (1995). Détermination de l'âge des thons tropicaux à partir de leurs otolithes: exemple du Yellowfin (*Thunnus albacares*). *Document Technique du Centre ORSTOM de Brest*, 76:1–31.
- Stéquert, B. and Conand, F. (2004). Age and growth of bigeye tuna (*Thunnus obesus*) in the Western Indian Ocean. *Cybium*, 28(2):163–170.
- Stéquert, B., Rodriguez, J., Cuisset, B., and Le Menn, F. (2001). Gonadosomatic index and seasonal variations of plasma sex steroids in skipjack tuna (*Katsuwonus pelamis*) and yellowfin tuna (*Thunnus albacares*) from the Western Indian Ocean. *Aquatic Living Resources*, 14:313–318.
- Uchiyama, J. and Struhsaker, P. (1981). Age and growth of skipjack tuna, *Katsuwonus pelamis*, and yellowfin tuna, *Thunnus albacares* as indicated by daily growth increments of sagittae. *Fishery Bulletin*, 79:151–162.
- Viera, A. (2005). Study of the growth of Yellowfin tuna (*Thunnus albacares*) in the Indian Ocean based on length-frequency data from 2000 to 2004. *IOTC-WPTT*, 32:17p.
- Wang, Y.-G. (1998). Growth curves with explanatory variables and estimation of the effect of tagging. *Australian and New Zealand Journal of Statistics*, 40(3):299–304.

- Wild, A. (1986). Growth of yellowfin tuna, *Thunnus albacares*, in the Eastern Pacific Ocean based on otolith increments. *Inter-American Tropical Tuna Commission Bulletin*, 18(6):423–479.
- Wild, A. and Foreman, T. (1980). The relationship between otolith increments and time for yellowfin and skipjack tuna marked with tetracycline. *Inter-American Tropical Tuna Commission Bulletin*, 17(7):507–560.
- Wild, A., Wexler, J., and Foreman, T. (1995). Extended studies of increment deposition rates in otoliths of yellowfin and skipjack tunas. *Bulletin of Marine Science*, 57(2):555–562.
- Zhu, G., Xu, L., Zhou, Y., and Song, L. (2008). Reproductive Biology of Yellowfin Tuna *T. albacares* in the West-Central Indian Ocean. *Journal of Ocean University of China*, 7(3):327–332.
- Zudaire, I., Murua, H., Grande, M., Korta, M., Arrizabalaga, H., Areso, J., and Delgado-Molina, A. (2010). Reproductive biology of yellowfin tuna (*Thunnus albacares*) in the Western and Central Indian Ocean. *IOTC-WPTT*, 48:25p.

Appendix B: Growth parameters of yellowfin and bigeye tunas in the three oceans

Table B.1: Growth parameters of yellowfin tuna

| Region | Data type | Method | FL range | k | L_{∞} | t_0 | Reference | |
|-----------------------------------|------------------------------|--------------------------|------------------------------|--------------|--------------|---------|-------------------------------|-------|
| Indian | Otoliths | Von Bertalanffy | | 0.176 | 245.541 | 0.266 | Stequert et al., 1996 | |
| | Length-frequency | Gascuel Model | 30 to 135 | 0.86 | 162.7 | | Viera, 2005 | |
| Western Indian | Otoliths | Von Bertalanffy | 60 to 20 | 0.176 | 272.7 | -0.266 | Stequert et al., 1995 | |
| | Length-frequency | Von Bertalanffy | 60 to 144 | 0.88 | 154.77 | 1.16 | Lumineau, 2002 | |
| | | Gascuel model | | 30 to 144 | 0.8 | 150.9 | | 1.7 |
| | | | | | 2.25 | 136.34 | | |
| | | | 0.84 | 152.07 | | | | |
| Minicoy | Length-frequency | Von Bertalanffy | 27 to 137 | 0.32 | 145 | -0.34 | Mohan and Kunhikoya, 1985 | |
| | Scales | Von Bertalanffy | | 0.278 | 222.8 | | Yang, 1969 | |
| Atlantic | Dorsal spines | Von Bertalanffy | | 0.37 | 192.4 | -0.003 | Draganic and Pelzcarski, 1984 | |
| | Length-frequency | Von Bertalanffy | | 0.72 | 166.4 | | Fonteneau, 1981 | |
| | | | | 0.5 | | 189 | | |
| | Tagging | Von Bertalanffy | | 0.56 | 183.9 | | Miyabe, 1984 | |
| | | Von Bertalanffy | | 0.411 | 198.08 | | Bard and Diouf, 1989 | |
| | | | 0.485 | 152.59 | | | | |
| Western Atlantic | Dorsale spines | Von Bertalanffy | | 0.267 | 230.7 | -0.081 | Lessa and Duarte-Neto, 2004 | |
| | | | | 0.42 | 194.8 | | Le Guen and Sakagawa, 1972 | |
| Eastern Atlantic | Length-frequency | Von Bertalanffy | 63 to 170 | 0.42 | 194.8 | -0.748 | Gascuel et al., 1992 | |
| | | | 40 to 150 | 1.195 | 158.5 | | | |
| | | Gascuel model | 41.4 to 147.4 | 1.495 | 152.6 | | | |
| Gulf of Guinea | Tagging | Von Bertalanffy | 65 to 180 | 0.474 | 196.55 | 0.847 | Bard, 1984 | |
| Gulf of Guinea | Tagging and Length-frequency | Von Bertalanffy | | 0.864 | 166.4 | 1.292 | Fonteneau | |
| Dakar and Senegal | | | | 0.936 | 161.02 | | | |
| Venezuela | | | | 0.6 | 189 | | | |
| Brasil | Length-frequency | Von Bertalanffy | 65.88 to 160 | 0.884 | 155.069 | 0.957 | Gaertner and Pagavino, 1992 | |
| | | | 65 to 155 | 0.43 | 184.12 | -0.079 | | |
| | | | Africa | 63.07 to 180 | 0.566 | 189.04 | | 1.193 |
| Gulf of Guinea and North Carolina | Otoliths | Von Bertalanffy | 30 to 179 | 0.281 | 245.541 | 0.0423 | Shuford et al., 2007 | |
| | | | 70 to 148 | 1.72 | 148 | 2 | | |
| | | | Pacific | 72 to 149 | 1.888 | 149 | | 2.294 |
| Western Pacific | Scales | Von Bertalanffy | M: 58 to 119 F: 57 to 119 | 0.333 | 192.8 | | Huang et al., 1974 | |
| | | | | 0.386 | 174.9 | | Huang and Yang, 1973 | |
| | | | | 0.129 | 178.6 | | Li et al. 1995 | |
| | | | | 0.276 | 202.1 | 0 | Le Guen and Sakagawa, 1973 | |
| | | | | 0.372 | 174.9 | 0 | | |
| | Otoliths | Modified Von Bertalanffy | 45 to 70 | 0.39 | 199.6 | -0.177 | Lehodey and Leroy, 1999 | |
| | | | | 0.728 | 151.7 | -0.085 | | |
| | | | | M: 0.805 | 146.7 | -0.049 | | |
| | Length-frequency | Von Bertalanffy | 0.25 | F: 0.511 | 177.1 | -0.167 | Hampton, 2000 | |
| | | | | 0.392 | 175 | 0.00306 | | |
| 0.66 | | | | 150 | 0.4 | | | |
| 0.292 | | | | 180.9 | 0 | | | |
| 0.52 | | | | 175.9 | 0.19 | | | |
| Eastern Central Pacific | Length-frequency | Von Bertalanffy | 93 to 167 | 0.45 | 180 | | Zhu et al. 2011 | |
| | | | | 0.66 | 167 | | | |
| Western coast of America | Increment technic | Von Bertalanffy | 80 to 140 | 0.36 | 214 | | Diaz, 1963 | |
| | | | | 0.7 | 166 | | | |
| | | | | 0.44 | 192 | 0.22 | | |
| Hawaii | Weight modes | Von Bertalanffy | 70 to 120 | 0.55 | 168 | 0.35 | Moore, 1951 | |
| Japanese | Length-frequency | Von Bertalanffy | 30 to 150 | 0.29 | 179 | | Yabuta and Yukinawa, 1957 | |
| Philippine waters | Length-frequency | Von Bertalanffy | 20 to 60 | 0.25 | 189 | | | |
| | | | 20 to 60 and 90 to 150 | 0.43 | 182 | | | |
| | | | 20 to 70 | 0.2 | 169 | | | |
| | | Von Bertalanffy | 20 to 60 and 120 to 160 | F: 0.32 | 173 | | Yesaki, 1983 | |
| | | | | M: 0.3 | 175 | | | |

Table B.2: Growth parameters of bigeye tuna

| Region | Data type | Method | FL range | k | L_{∞} | t_0 | Reference |
|----------------------|---------------------------------|-----------------------------|---------------|----------------------|--------------|-------------------------|----------------------------------|
| Indian | | Von Bertalanffy | | F: 0.171 M: 0.058 | 209.8 423 | -0.86 -1.773 | Tankevich, 1992 |
| | Otoliths and first dorsal spine | Generalized Von Bertalanffy | 59 to 147 | 0.32 | 169.06 | -0.34 | Stéquert & Conand, 2004 |
| | Length-frequency | Von Bertalanffy | 36 to 190 | 0.35 | 223.288 | -0.02 | Chantawong et al., 1999 |
| Atlantic | Ray of dorsal fin | Von Bertalanffy | 50 to 200 | 0.173 | 253.8 | -0.15 | Gaiko et al., 1980 |
| | | | 50 to 190 | 0.23 | 218.8 | -0.02 | Draganik & Pelczarski, 1984 |
| | | | 58 to 187 | 0.182 | 206.1 | -0.74 | Delgado de Molina & Santan, 1986 |
| | Length-frequency | Von Bertalanffy | | 0.0135 | 491.6 | 3.808 | Weber, 1980 |
| | | | 35 to 190 | 0.085 | 381.5 | -0.4 | Pereira, 1984 |
| Eastern Atlantic | Otoliths | Gompertz | 29 to 190 | | 179.13 | | Hallier et al., 2005 |
| | | Richards | | | 178.63 | | |
| | | Von Bertalanffy | | 0.202 | 207.43 | -0.613 | |
| | Otoliths and tagging | Von Bertalanffy | | 0.18 | 217.28 | -0.709 | |
| | Tagging | | 37 to 124 | 0.206 | 195.54 | | |
| | Tagging | Von Bertalanffy | 40 to 150 | 0.113 | 285.4 | -0.5 | Cayré & Diouf, 1984 |
| | Length-frequency | Von Bertalanffy | 61 to 139 | 0.104 | 338.5 | -0.54 | Champagnat & Pianet, 1974 |
| | | | 45 to 150 | 0.149 | 259.6 | -0.4 | Marcille et al., 1978 |
| Pacific | Scales | Von Bertalanffy | 58 to 109 | 0.11 | 195.2 | -1.13 | Nose et al., 1957 |
| | | | 60 to 150 | 0.21 | 215 | -0.01 | Yukinawa & Yabuta, 1963 |
| | Length-frequency | Von Bertalanffy | 65 to 150 | 0.16 | 257.5 | -0.11 | |
| | Tagging | Von Bertalanffy | | 0.37 | 165.3 | -0.34 | Kirkwood, 1983 |
| Otoliths | Von Bertalanffy | 25 to 157 | 0.266 | 203.59 | -0.394 | | |
| Otoliths and tagging | Composite Von Bertalanffy | 25 to 185 | 0.349 | 166.3 | -0.389 | Lehodey et al., 1999 | |
| Tagging | Von Bertalanffy | 30 to 185 | 0.226 | 228.59 | -0.425 | | |
| Western Pacific | Length-frequency | Von Bertalanffy | 80 to 155 | F: 0.32 | 183 | -0.72 | Shomura & Keala, 1963 |
| | | | | M: 0.27 | 196.7 | -0.93 | |
| | Otoliths | Von Bertalanffy | 39 to 178 | 0.24 | 169.09 | -1.71 | Farley et al., 2006 |
| | Otoliths and tagging | Von Bertalanffy | 25 to 175 | 0.37 | 165.3 | 0.34 | Hampton & Leroy, 1998 |
| Eastern Pacific | Tagging | Von Bertalanffy | | 0.254 | 184 | | Hampton et al., 1998 |
| | | | | 0.427 | 156.82 | 0.53 | |
| | First dorsal spine | Von Bertalanffy | 45.5 to 189.2 | F: 0.191 | 211.4 | -0.459 | Sun et al., 2001 |
| | | | | M: 0.179 | 220.6 | -0.557 | |
| | | | | F+M: 0.184 | 216.1 | -0.527 | |
| | | | | All: 0.185 | 226.4 | -0.446 | |
| | Length-frequency | Von Bertalanffy | | All: 0.201 | 208.7 | -0.991 | Suda & Kume, 1967 |
| 0.21 | | | | 214.8 | -0.02 | | |
| Weigth-frequency | Modified Von Bertalanffy | | 0.465 | 157.9 | -0.003 | Kikkawa & Cushing, 2001 | |
| | | | 0.395 | 165.7 | -0.004 | | |
| | | | 0.224 | 204.9 | -0.005 | | |
| | | | 0.201 | 204.1 | -0.006 | | |
| | | | 0.319 | 177.6 | -0.004 | | |
| | | | 0.246 | 189.8 | -0.005 | | |
| Otoliths | Von Bertalanffy | 30 to 149 | 0.307 | 181.2 | -0.004 | Schaefer & Fuller, 2006 | |
| | | | F: 0.079 | 513.8 | -0.458 | | |
| | | | M: 0.099 | 418.9 | -0.477 | | |
| | | | All: 0.108 | 400.3 | -0.398 | | |
| Tagging | | 30 to 150 | 0.12 | 367.7 | | | |
| Length-frequency | Von Bertalanffy | 82 to 150 | 0.095 | 186.95 | 2.11 | Kume & Joseph, 1966 | |
| | | 50 to 198 | 0.23 | 207.4 | -0.43 | | |
| | | 85 to 192 | F: 0.32 | 207.4 | -0.44 | Zhu et al., 2009 | |
| | | 75 to 198 | M: 0.27 | 202.1 | -0.44 | | |

Appendix C: Presentation of mark-recapture data

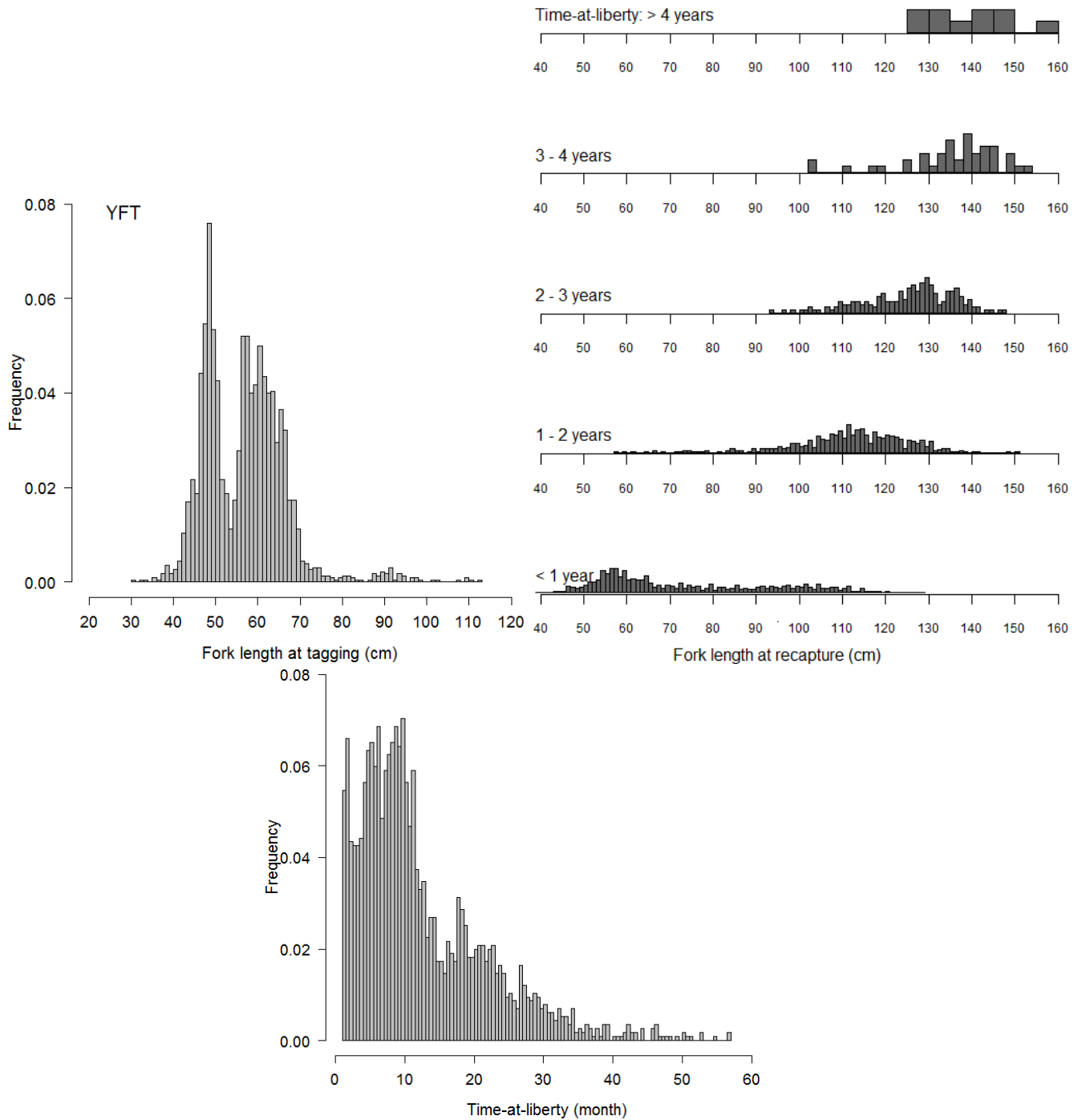


Figure C.1: Mark-recapture dataset for yellowfin

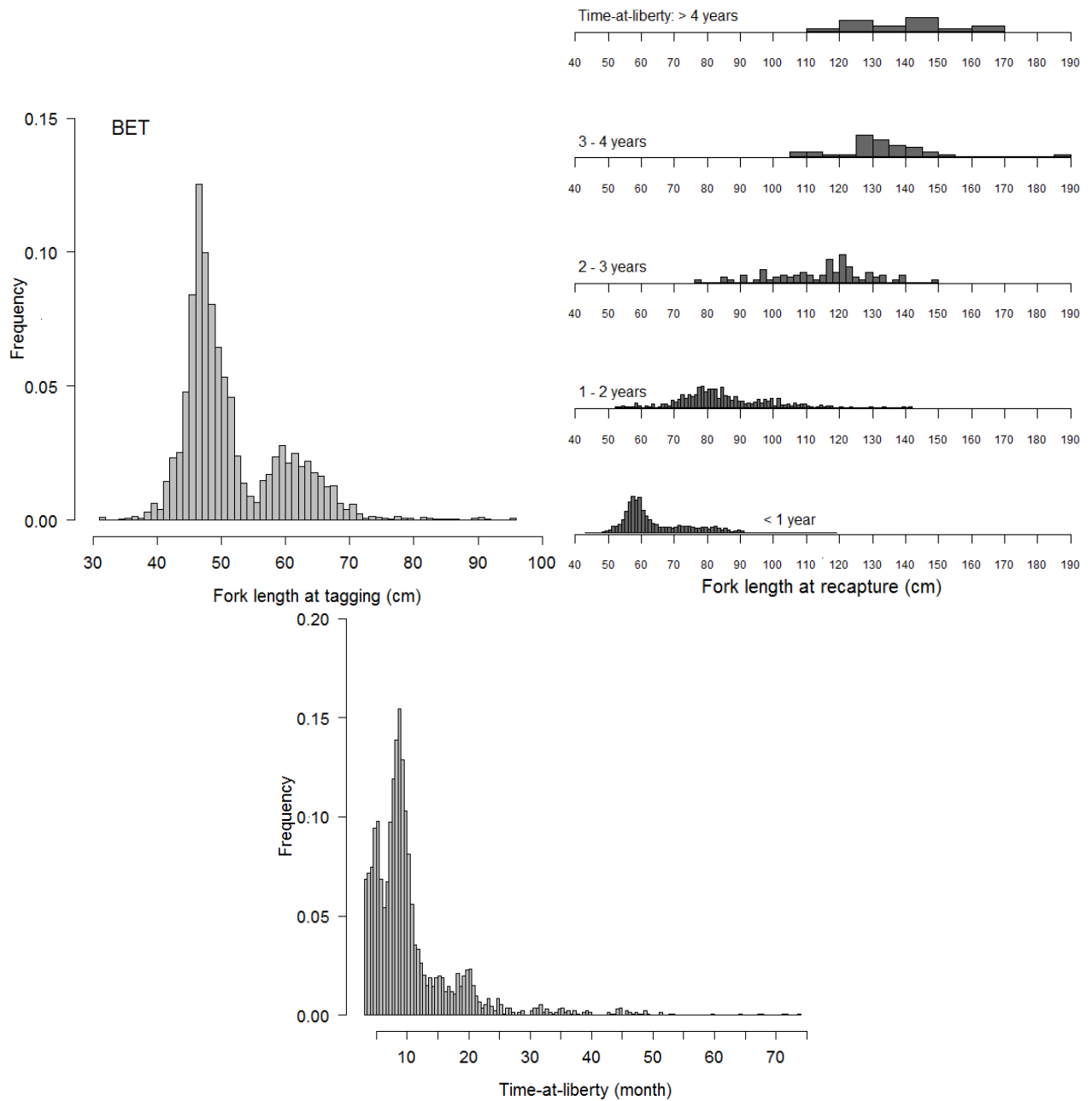


Figure C.2: Mark-recapture dataset for bigeye